Journal of Visualized Experiments

Confocal Laser Scanning Microscopy of Calcium Dynamics in Acute Mouse Pancreatic Tissue Slices

--Manuscript Draft--

Article Type:	Invited Methods Collection - JoVE Produced Video
Manuscript Number:	JoVE62293R1
Full Title:	Confocal Laser Scanning Microscopy of Calcium Dynamics in Acute Mouse Pancreatic Tissue Slices
Corresponding Author:	Masa Skelin Institute of Physiology, Faculty of Medicine University of Maribor in Slovenia: Univerza v Mariboru Medicinska fakulteta Maribor, SLOVENIA
Corresponding Author's Institution:	Institute of Physiology, Faculty of Medicine University of Maribor in Slovenia: Univerza v Mariboru Medicinska fakulteta
Corresponding Author E-Mail:	masa.skelin@um.si
Order of Authors:	Andraž Stožer
	Jurij Dolenšek
	Lidija Križančić Bombek
	Viljem Pohorec
	Marjan Slak Rupnik
	Masa Skelin Klemen
Additional Information:	
Question	**Response**
Please specify the section of the submitted manuscript.	Biology
Please indicate whether this article will be Standard Access or Open Access.	Open Access (US$4,200)
Please indicate the **city, state/province, and country** where this article will be **filmed**. Please do not use abbreviations.	Maribor, Slovenia
Please confirm that you have read and agree to the terms and conditions of the author license agreement that applies below:	I agree to the Author License Agreement
Please provide any comments to the journal here.	

TITLE:

Confocal Laser Scanning Microscopy of Calcium Dynamics in Acute Mouse Pancreatic Tissue Slices

AUTHORS AND AFFILIATIONS:

Andraž Stožer[1], Jurij Dolenšek[1,2], Lidija Križančić Bombek[1], Viljem Pohorec[1], Marjan Slak Rupnik[1,3], Maša Skelin Klemen[1*]

[1]Institute of Physiology, Faculty of Medicine, University of Maribor, Maribor, Slovenia
[2]Faculty of Natural Sciences and Mathematics, University of Maribor, Maribor, Slovenia
[3]Center for Physiology and Pharmacology, Medical University of Vienna, Vienna, Austria

Emails of co-authors:

Andraž Stožer	(andraz.stozer@um.si)
Jurij Dolenšek	(jurij.dolensek@um.si)
Lidija Križančić Bombek	(lidija.bombek@um.si)
Viljem Pohorec	(viljem.pohorec@um.si)
Marjan Slak Rupnik	(marjan.slakrupnik@meduniwien.ac.at)

***Corresponding author:**

Maša Skelin Klemen	(Masa.skelin@um.si)

KEYWORDS:

Pancreas, agarose, tissue slice, in situ preparation, confocal laser scanning microscopy, calcium imaging, single-cell resolution, 3R

SUMMARY:

We present the preparation of acute pancreatic tissue slices and their use in confocal laser scanning microscopy to study calcium dynamics simultaneously in a large number of live cells, over long time periods, and with high spatiotemporal resolution.

ABSTRACT:

The acute mouse pancreatic tissue slice is a unique in situ preparation with preserved intercellular communication and tissue architecture that entails significantly fewer preparation-induced changes than isolated islets, acini, ducts, or dispersed cells described in typical in vitro studies. By combining the acute pancreatic tissue slice with live-cell calcium imaging in confocal laser scanning microscopy (CLSM), calcium signals can be studied in a large number of endocrine and exocrine cells simultaneously, with a single-cell or even subcellular resolution. The sensitivity permits the detection of changes and enables the study of intercellular waves and functional connectivity as well as the study of the dependence of physiological responses of cells on their localization within the islet and paracrine relationship with other cells. Finally, from the perspective of animal welfare, recording signals from a large number of cells at a time lowers the number of animals required in experiments, contributing to the 3R—replacement, reduction, and refinement—principle.

INTRODUCTION:

The mammalian pancreas is a large exocrine and endocrine gland. The exocrine part makes up 96–99% of the total pancreas volume and consists of acini and ducts. The endocrine part is made up of a large number of islets of Langerhans accounting for the remaining 1–4% of the total pancreas volume[1]. The exocrine part secretes major digestive enzymes that break down energy-rich polymers in food, as well as a bicarbonate-rich fluid, which combines with other gastrointestinal secretions to provide an environment suitable for the action of enzymes. The endocrine part secretes hormones that regulate postprandial distribution, storage, and interprandial release of energy-rich nutrients. Although the exocrine tissue is relatively underdeveloped and the endocrine relatively well-developed at birth, the former quickly overgrows the latter upon weaning[2-4]. Early studies of pancreatic function marked the birth of modern physiology, and major methodological advancements in the field have been followed by major scientific breaktroughs[5]. Working with the pancreas is technically challenging due to the intricate structure of the gland, but is also a big motivation because of diseases such as pancreatic cancer, pancreatitis, and diabetes that present major threats to public health, and for which novel therapeutic approaches are needed.

Isolated islets[6], acini[7,8], and ductal fragments had been developed and used for decades as gold standard methods owing to their advantages compared with cell lines and primary dispersed endocrine, acinar, and ductal cells[9,10]. Despite the markedly improved function of isolated cell collectives, these methods still involve considerable mechanical and enzymatic stress, isolate cells from the surrounding tissue and thus lack paracrine interactions and mechanical support, and most importantly, are accompanied by significant changes to normal physiology[11-13]. The acute mouse pancreatic tissue slice was developed in 2001 out of a perceived need to develop an experimental platform similar to brain, pituitary, and adrenal slices with preserved intercellular contacts, paracrine interactions, mesenchyme, and tissue architecture, as well as without some of the most important shortcomings of the gold standard method in islet research of that time—the isolated islets[12,14]. Among these shortcomings are damage to the outermost layers, lack of accessibility of core islet areas, and the need for cultivation with possibly important effects on cell identity and physiology[12,15]. Moreover, the tissue slice method enables studies on animal models with grossly deranged islet architecture where it is impossible to isolate islets, or when islet yield is extremely low by traditional isolation[16-21].

Additionally, the slice is more suitable for studying morphological changes during the development of diabetes and pancreatitis, for instance, as it enables a better overview of the whole tissue and is also compatible with studying regional differences. Importantly, despite the early focus on the endocrine part, the tissue slice method inherently enables the study of the exocrine components[9,22,23]. During the first decade after its introduction, the method was employed for electrophysiological studies of beta[14,24-29] and alpha[30,31] cells as well as for examining the morphological and functional maturation of the pancreas[2,3]. A decade later in 2013, the method was successfully adapted for live-cell calcium imaging of islet cells using CLSM to characterize their responses to glucose[32], their functional connectivity patterns[33], and the relationship between membrane potential and intracellular calcium by combining a fluorescent calcium dye with a membrane potential dye[34]. Later in the same year, the method was also used

to assess calcium dynamics in acinar cells[22,35]. Over the following years, pancreatic tissue slices have been used in a number of different studies and successfully adapted to pig and human tissue[9,36-41]. However, taken together, calcium imaging—in mouse pancreatic tissue slices in general and in islets in particular—is still mostly performed by this group. One of the main reasons for this may lie in the combination of a technically challenging tissue slice preparation, the need for a confocal microscope, and rather complex data analysis. The main aim of the present paper is to make this powerful method more accessible to other potential users.

There are already some excellent methodological articles dealing in detail with tissue slice preparation and the use of slices for structural and secretion studies, but not for confocal calcium imaging[9,42,43]. Therefore, this paper focuses on some additional tips and tricks during the preparation of slices, on steps critical for successful dye loading, image acquisition, as well as on the main steps of basic calcium data analysis. Therefore, this contribution should be viewed as being complementary to rather than as an alternative for the abovementioned method. Similarly, calcium imaging in mouse pancreatic tissue slices shall be viewed as an experimental approach to be used to answer specific questions and is thus complementary to rather than an absolute alternative for other calcium imaging approaches in pancreatic physiology such as isolated ducts or acini, isolated islets, organoids, islets transplanted into the anterior chamber of the eye, and recordings in vivo[11,44-48]. The promise of calcium imaging in mouse pancreatic tissue slices is probably best illustrated by recent successful recordings of calcium dynamics in islet mesenchymal cells such as pericytes[49] and macrophages[50], as well as in ductal cells[23].

PROTOCOL:

NOTE: All experiments were performed in strict accordance with institutional guidelines for the care and use of animals in research. The protocol was approved by the Administration of the Republic of Slovenia for Food Safety, Veterinary Sector and Plant Protection (permit number: 34401-35-2018/2).

1. Preparation of pancreatic tissue slices

NOTE: The preparation of acute mouse pancreas tissue slices for calcium imaging using CLSM requires a number of instruments, different solutions, and proceeds in a series of critical steps that are schematically presented in **Figure 1** and described in detail below.

Insert **Figure 1** here.

1.1. Preparation of solutions

NOTE: All solutions should be prepared in advance and can be stored in the refrigerator at 4–8 °C for up to one month. For the preparation and storage of tissue slices, approximately 0.5 L of extracellular solution (ECS) with 6 mM glucose and 0.3 L of 4-(2-hydroxyethyl)-1-piperazineethanesulfonic acid (HEPES) buffer is needed. For 1 day of calcium imaging with the perifusion system set at 1–2 mL/min flow rate, approximately 0.5 L of ECS is needed.

1.1.1. Extracellular solution with 6 mM glucose

1.1.1.1. Prepare 1 L of ECS containing 125 mM NaCl, 26 mM $NaHCO_3$, 6 mM glucose, 6 mM lactic acid, 3 mM myo-inositol, 2.5 mM KCl, 2 mM Na pyruvate, 2 mM $CaCl_2$, 1.25 mM NaH_2PO_4, 1 mM $MgCl_2$, and 0.5 mM ascorbic acid. Mix thoroughly until all ingredients completely dissolve. Take 50 μL of ECS into an 0.5 mL microcentrifuge tube, place it onto the osmometer according to the manufacturer's instructions, and check the osmolarity.

NOTE: The osmolarity should be 300–320 mOsm. For stimulation of beta cells, use solutions with higher glucose concentrations. To ensure physiological pH value of 7.4 during slicing and experiments, constantly bubble the ECS with carbogen (i.e., a gas mixture of 95% O_2 and 5% CO_2) at barometric pressure. A simple bubbling system can be set up by attaching one end of a 5 mm silicon tubing to the source of carbogen (i.e., a pressurized gas cylinder) and the other end of the tubing placed directly into the bottle containing ECS.

1.1.1.2. Alternatively, prepare a 10x stock containing 1250 mM NaCl, 260 mM $NaHCO_3$, 30 mM myo-inositol, 25 mM KCl, 20 mM Na pyruvate, 12.5 mM NaH_2PO_4, and 5 mM ascorbic acid. When the ECS containing 6 mM glucose is needed, mix 100 mL of the stock with 2 mL of 1 M $CaCl_2$, 1 mL of 1 M $MgCl_2$, 0.455 mL of 13.2 M lactic acid, and 1.08 g of glucose, and fill with double-distilled water up to 1 L. If needed, use different amounts of glucose to obtain other glucose concentrations.

1.1.2. HEPES buffer with 6 mM glucose

1.1.2.1. Prepare 0.5 L of HEPES-buffered solution (HBS) containing 150 mM NaCl, 10 mM HEPES, 6 mM glucose, 5 mM KCl, 2 mM $CaCl_2$, and 1 mM $MgCl_2$; titrate to pH = 7.4 with 1 M NaOH.

NOTE: If carbogen is not available, this buffer can be used for all steps instead of ECS.

1.1.3. Agarose (1.9% w/w)

1.1.3.1. Prewarm a water bath to 40 ˚C.

1.1.3.2. Add 0.475 g of low-melting-point agarose and 25 mL of ECS containing 6 mM glucose to an Erlenmeyer flask, and place the flask in a microwave oven at maximum power for a few seconds until it starts to boil. Take the flask out of the oven and swirl it a few times, until the agarose dissolves completely. Transfer the flask with the liquid agarose to the prewarmed water bath at 40 ˚C to cool the agarose to the desired temperature and to keep it liquid until injection. Secure the flask with a stabilizing lead ring.

NOTE: The agarose can be prepared in advance and kept in the refrigerator. Before use, warm the agarose in the microwave oven until it liquefies, and transfer the Erlenmeyer flask into a

water bath prewarmed to 40 °C. The agarose can be re-used up to 5x. If re-used beyond 5x, it will become dense and harder to inject.

1.2. Injection of pancreas with agarose

NOTE: Sections 1.2 and 1.3 explain the preparation of tissue slices that can be used for different experimental purposes such as calcium imaging, electrophysiology, immunohistochemistry, secretion studies, and structural/microanatomical studies.

1.2.1. Fill a 5 mL syringe with the liquid agarose from the Erlenmeyer flask in the water bath from step 1.1.3.2, remove any bubbles, and mount a 30 G needle. Protect the needle with a cap, and keep the filled syringe back in the water bath with the needle facing downward and the entire volume of agarose below the water surface. Secure the syringe with a stabilizing lead ring in such way that the ring presses the syringe against the wall of the water bath.

NOTE: Be careful not to push any agarose into the needle as it will harden quickly and block the needle. If the room temperature is low, and if the injection is performed by a less experienced person, increase the temperature of the water bath up to 42 °C to gain some additional time for injection.

1.2.2. Fill an ice bucket with ice, and place the bottle containing ECS in it. Bubble the ECS constantly at 1.5 mL/min with carbogen at barometric pressure and room temperature to ensure oxygenation and a pH of 7.4.

1.2.3. Sacrifice a mouse by administering a high concentration of CO_2 followed by cervical dislocation. Make all efforts to minimize animal suffering.

1.2.4. Working under a stereomicroscope, access the abdomen via laparotomy (**Figure 2A**). Gently flip the gut to the left side of the mouse (from the anatomical perspective of the mouse) to expose the common bile duct. Use forceps to slightly lift the duodenal part, and find the major duodenal papilla—papilla of Vater. Clamp the common bile duct at the duodenal papilla using a hemostat (**Figure 2B,C**) to prevent leakage of agarose from the duct into the duodenum.

NOTE: To prevent agarose leakage into the duodenum and further up and down in the gastrointestinal tract, place the hemostat in such a way that it also clamps the duodenum both proximally and distally from the papilla. It is best to use a curved hemostat for this purpose.

1.2.5. With small sharp forceps, reach under the common bile duct, and break the membrane that attaches the duct to the pancreatic tissue. For better visual control and easier injection, clear as much fat and connective tissue from the duct as possible.

1.2.6. Place the duct perpendicularly onto large forceps (**Figure 2D**), and inject the prepared liquid agarose into the proximal part of the common bile duct (**Figure 2D**). Be sure to squeeze the syringe hard as the agarose is viscous. Keep filling the pancreas until it becomes whitish and

slightly distended or for at least 20–30 s.

NOTE: This is the most critical step in slice preparation. If there are any kinks in the ductal tree of the pancreas, gently elevate or pull the pancreas away from the syringe to level them out. Do not decide when to stop injection based on the volume injected from the syringe as the backflow at the point of injection and forward leakage into the duodenum are typically much higher than the volume injected into the ductal tree of the pancreas. Importantly, successful injections can be performed with practically unnoticeable changes in syringe volume.

1.2.7. Remove the syringe, and slowly pour 20 mL of the bubbled ice-cold ECS at 0–4 °C from the bottle onto the pancreas to cool the tissue and harden the agarose.

1.2.8. Gently extract the pancreas using forceps and fine tough-cut scissors. Place the extracted pancreas into a 100 mm Petri dish containing ~40 mL of ice-cold ECS, and gently move it around to wash it. Transfer the pancreas into a fresh 100 mm Petri dish containing ~40 mL of ice-cold ECS.

1.2.9. From the well-injected part of the pancreas, which appears whitish (**Figure 3A**), cut up to 6 blocks of tissue, 0.1–0.2 cm^3 in size, using forceps and tough-cut scissors. Clear them of any connective and fatty tissue.

1.2.10. Fill a 35 mm non-sticky bottom-Petri dish with approximately 5 mL of liquid agarose at 40 °C, transfer the tissue blocks into it, and immediately put the Petri dish on ice to cool it down and harden the agarose.

NOTE: The way the blocks of pancreas are trapped in agarose determines the way they are cut during slicing. Experienced experimentalists can try and fine-tune the position of the blocks during the few moments before the agarose hardens when placed on ice.

1.2.11. After the agarose with the tissue blocks hardens, turn the Petri dish upside down onto a flat smooth surface such as the lid of a 100 mm Petri dish, and remove the agarose by gently cutting with one half of a razor blade into the margin between the lateral wall of the Petri dish and the agarose. With a razor blade, cut individual agarose cubes, each containing one tissue block, taking care that each tissue block is surrounded by agarose. Glue the agarose blocks onto the sample plate of the vibratome with cyanoacrylate glue (**Figure 3B**).

Insert **Figure 2** here.

1.3. Slicing

1.3.1. Fill the cutting chamber of the vibratome with ~0.15 L of ice-cold ECS, and bubble constantly with carbogen. Surround the cutting chamber with ice, and add 2 ice cubes (~10 mL each) made of ECS with 6 mM glucose into the cutting chamber. Mount the razor blade for cutting onto the vibratome, and screw-fix the sample plate with agarose blocks into its place.

1.3.2. Set the slicer to cut agarose blocks at 0.05 to 1 mm/s and 70 Hz into 140 µm-thick slices with a surface area of 20–100 mm^2. For slicer settings, follow the manufacturer's instructions.

1.3.3. Immediately after each cutting step, pause the slicer, gently collect the slices with a fine paint brush, and transfer them into a 100 mm Petri dish filled with 40 mL of HEPES buffer with 6 mM glucose at room temperature (**Figure 3C**).

NOTE: The slices can be kept in HEPES buffer at room temperature for at least 12 h, and the buffer should be exchanged every 2 h.

Insert **Figure 3 here.**

2. Live/dead assay using LIVE/DEAD Viability/Cytotoxicity Kit for mammalian cells

NOTE: For some experiments, it is useful to check the viability of cells in the slices (**Figure 4**) by the live/dead assay as follows.

2.1. Follow the manufacturer's instructions to thaw vials with reagents of the LIVE/DEAD Viability/Cytotoxicity Kit, and prepare working solutions of calcein AM just before use. Use the solutions within one day.

2.2. In a 15 mL centrifuge tube, mix 5 µL of 4 mM calcein AM (Component A), 20 µL of 2 mM ethidium homodimer-1 (EthD-1, Component B), and 10 mL of Dulbecco's Phosphate-buffered Saline (D-PBS) to prepare a working solution containing approximately 2 µM calcein AM and 4 µM EthD-1. Vortex thoroughly.

2.3. Using a fine paint brush, gently transfer the tissue slices into a 3 mL Petri dish with fresh HEPES buffer to dilute serum esterase activity. Remove the HEPES buffer, and cover the slices with 100–200 µL (or more if necessary) of the working solution from step 2.2.

2.4. Incubate the slices for 30–45 min at room temperature in a closed Petri dish. Image the tissue slices using excitation/emission filters as recommended by the manufacturer.

3. Calcium dye loading

NOTE: Fluorescent dyes should be shielded from light exposure during the whole process of preparation and loading of the dye, as well as during handling of the stained tissue slices. Tin foil can be used to cover tubes or Petri dishes containing the calcium dye.

3.1. Dye preparation

3.1.1. Dissolve the contents of one vial (50 µg) of the cell permeable Ca^{2+} indicator dye

(excitation/emission 495/523 nm; see the **Table of Materials**), 7.5 µL of dimethylsulfoxide (DMSO), and 2.5 µL of the polaxamer (20% solution in DMSO; **Table of Materials**) in 6.667 mL of HBS containing 6 mM glucose in a 15 mL screw cap tube.

NOTE: This final solution contains 6 µM of the Ca^{2+} indicator dye, 0.11% DMSO, and 0.037% polaxamer.

3.1.2. Aspirate and expel the solution in the screw cap tube repeatedly with a pipette for 20 s; submerge the tube in an ultrasonic bath chamber for 30 s, and vortex for 30 s to improve solubilization. Aliquot 3.333 mL of the final Ca^{2+} indicator dye solution prepared in step 3.1.1 into 5 mL Petri dishes.

3.2. Dye loading

3.2.1. Transfer the prepared tissue slices from the 60 mL Petri dish with HBS into 5 mL Petri dishes filled with the dye solution by gently lifting each tissue slice using a thin, soft paint brush and placing it in the dye solution. Incubate up to 10 tissue slices per Petri dish.

3.2.2. Place the slice-loaded Petri dish on an orbital shaker at room temperature set to orbital motion at 40 turns per minute for 50 min. Incubate the slices in the dye solution exposed to ambient air at room temperature, but shielded from light by covering the Petri dish with tin foil.

3.3. Storing of slices

3.3.1. Transfer the stained tissue slices from the 5 mL Petri dish into a 60 mL Petri dish filled with dye-free HBS by gently lifting them using a fine, soft paint brush. Store up to 20 slices per Petri dish.

NOTE: Use the tissue slices for imaging at this point. The tissue slices will retain the Ca^{2+} indicator dye for several hours. The survival of slices and retention of the dye can be improved by placing the Petri dish in an insulated container, surrounded by ice. This is especially important if the dye-loaded slices are to be transported. Additionally, exchange the HBS every 2 h.

4. Calcium imaging

4.1. Setup of the confocal microscope

4.1.1. Choose an appropriate objective magnification depending on the interest of the study. Select 20x and 25x (numerical aperture [NA] 0.77–1.00) for visualizing a whole islet, several acini simultaneously, or larger ducts. Select higher magnifications to study intracellular dynamics.

4.1.2. Choose the acquisition mode for time-lapse imaging (e.g., **time-lapse**, **xyt**, or similar mode). Set the pinhole to 100–200 µm.

4.1.3. Set the light path for green fluorophores: excitation at 488 nm, and collection of emission at 500–700 nm. Preferably select detectors with a high quantum efficiency (e.g., gallium arsenide phosphide) over photomultiplier detectors.

4.2. Setup of the recording chamber and the perifusion system

4.2.1. Mount the recording chamber on the temperature-controlled stage of the microscope and the perifusion system (either gravity-fed or peristaltic-pump-based setup, volume 1 mL). Position the inlet and the outlet on the far edges of the recording chamber to avoid meandering of the perfusate within the chamber, and set the inflow and the outflow to equal values (1–2 mL/min). Avoid drifting of the liquid meniscus height and droplets in the perifusate.

4.2.2. Set the temperature control of the perifusion system to 37 °C. Initiate the perifusion with the non-stimulatory solution, and prepare the stimulating solutions. Change the solutions via motorized valves or by manually switching the solutions that feed the perifusion system.

4.3. Record calcium dynamics

4.3.1. Transfer a single tissue slice into the recording chamber. Immobilize the tissue slice with a U-shaped platinum weight with taut nylon mesh (e.g., from nylon stockings). Avoid positioning nylon threads over the structure of interest.

4.3.2. Locate an islet/acinus/duct using the brightfield option. Run live imaging to position the studied structures into the field of view, and set up the imaging parameters. Optimize the signal-to-noise ratio by adjusting the laser power, detector amplification, and line averaging/binning to allow visualization of the cells while keeping the laser power minimal.

4.3.3. Adjust the focal plane of the recording to ~15 µm below the cut surface (**Figure 5**) to avoid recording from potentially damaged cells at the cut surface.

4.3.4. Acquire images. Set the sampling frequency to 1–2 Hz to detect individual oscillations initially, and use a resonant scanner capable of fast line averaging (8–20) at a higher acquisition rate (>10 Hz) to record intracellular Ca^{2+} ($[Ca^{2+}]_{IC}$) activity. Allow an interval (e.g., 30% of the total sampling time) between consecutive point illuminations to prevent phototoxicity. Record a high-resolution image (e.g., 1024 x 1024 pixels, line averaging > 50) before the time series acquisition (see section 5).

NOTE: The sampling frequency of 1–2 Hz is below the Nyquist criterion for acquisition frequency for most cells, and the shape of the signal will be undersampled by default.

4.3.5. Refer to an online chart, if available in the imaging software, to obtain instant feedback on the preparation response, over-illumination, photobleaching, and mechanical drift. In case of a high rate of bleaching during acquisition, stop the recording and decrease laser power while increasing the detector gain to maintain the signal-to-noise ratio. In the case of mechanical drift,

check for tension between tubing/cables and the microscope stage as well as liquid leakage or changes of the volume in the recording chamber. Optionally, attempt to correct the drift during acquisition manually; however, note that this will inherently yield limited results.

NOTE: Endocrine cells are highly heterogeneous at near-threshold concentrations. A sufficient length of stimulation is needed to detect the range of activation/deactivation delays in individual cells. This is especially important for accurate detection of off-responses following highly stimulatory protocols.

4.3.6. Use calcium imaging to functionally discriminate between endo- and exocrine cells (**Figure 6**). To record transient activity during activation and deactivation, apply stimuli without stopping the recording.

4.3.7. Save the data after the end of experimentation (consider using an auto-save function). Allow a cooling period before switching off the laser power so as not to damage the lasers during the shutdown procedure.

5. Analysis of data

5.1. Visually inspect the recording qualitatively by replaying the time-lapse video. Check for cell drifts from the field of view or the optical plane. If a drift within the optical plane has occurred, employ the drift correction plugin in ImageJ.

5.2. Select regions of interest (ROIs) using microscope software or third-party software. Use the high-resolution image, maximal projection, or frame average as the reference to select ROIs. Replay the time-lapse imaging to visualize responding cells that are not visible in reference images. Position the ROIs such that the selected area of a ROI does not overlap with neighboring cells to avoid signal crosstalk between ROIs.

5.3. Export the time series data as ROI average value per frame. Export ROI coordinates.

5.4. Correct the time series data for bleaching (**Figure 7A**) by employing a combination of an exponential and linear fit, as described by

$$xcorr(t) = a \cdot e^{-b \cdot x(t)} + c \cdot x(t) \qquad (1)$$

where *x(t)* denotes the fluorescence signal at a time point *t*; *xcorr(t)* the corrected signal at the corresponding time points; and *a*, *b*, and *c* the parameters of the fit calculated as the least sum of squares between the *corr(t)* and *x(t)*.

5.5. Analyze the activation and deactivation phase of the response (**Figure 7B**). Calculate the first derivative of the time series data, and determine the zenith and the nadir of the derivative corresponding to the activation and deactivation, respectively. Alternatively, manually select the start of the phasic increase. Save and export the activation/deactivation times and corresponding

cell coordinates.

5.6. Analyze the plateau phase (**Figure 7C**). Detect individual oscillations by thresholding the raw data or by thresholding the first derivative of the time-series data. Define the beginning and end of an individual oscillation as the time corresponding to the oscillation's half amplitude.

5.6.1. Calculate the duration and the frequency of individual oscillations for each cell. Calculate the inverse value of the interspike interval (suitable for regular activity patterns). Alternatively, divide the number of oscillations by the time interval of the record (suitable for irregular activity patterns).

5.6.2. Calculate the active time. Express the active time as the sum of durations, and divide this value by the time interval. Alternatively, multiply the frequency and the duration that correspond with an oscillation.

NOTE: Dividing the sum of durations by the time interval provides robust results, but has low statistical discrimination as a single data point per cell is obtained. Multiplying the frequency and duration of an oscillation provides an oscillation-to-oscillation temporal resolution.

REPRESENTATIVE RESULTS:

The injection of the agarose solution into the pancreatic duct is the most critical step in pancreas tissue slice preparation. A successful injection can be recognized by a whitening of the pancreas tissue, as seen on the left side of **Figure 3A**, while an incompletely injected part of the pancreas is presented on the right side of **Figure 3A**. The islets of Langerhans can be recognized by the naked eye or under a stereomicroscope, and this aids in cutting the appropriate parts of the pancreas for subsequent embedding in agarose blocks (**Figure 3B**). In a freshly cut mouse pancreatic tissue slice, islets of Langerhans can be easily distinguished from the surrounding exocrine tissue and mesenchyme as white spots under the stereomicroscope (**Figure 3C**) or as brownish structures under the light microscope (**Figure 3D**). The pancreatic tissue slices can be used for distinct types of experiments for at least 12 h after slicing. In addition to the gross morphological assessment under the stereomicroscope, the light microscope, and the functional responses of cells during calcium imaging, the viability of the pancreatic tissue slices can be assessed (**Figure 4**).

Insert **Figure 4 here.**

For calcium imaging experiments, the fluorescent calcium indicator needs to penetrate through a few layers of cells. **Figure 5A** presents successful loading of the cell-permeable Ca^{2+} indicator dye into the pancreatic tissue slice in which individual islet and acinar cells can be recognized. In contrast, slices in **Figure 5B–D** are not optimal due to unsuccessful penetration of the dye (**Figure 5B**), lack of islet cells (**Figure 5C**), and a lot of necrotic tissue on the surface (**Figure 5D**). Such slices can be discarded, checked for the presence of additional islets that are cut or stained better (see **Table 1** for troubleshooting), or used for recording the responses of exocrine cells.

Insert **Figure 5 here.**

Representative results from calcium imaging using the cell-permeable Ca^{2+} indicator dye are shown in **Figure 6**. In **Figure 6A**, a high-resolution image of a pancreatic tissue slice is presented, containing an islet of Langerhans, acinar tissue, and a pancreatic duct. For better distinction, the endocrine, exocrine, and ductal part of the pancreatic tissue slice presented in **Figure 6A** are colored in **Figure 6B**. Using appropriate stimuli can functionally discriminate between different islet cells, or islet and non-islet cells[51]. Beta cells will typically respond to a square-pulse stimulation by glucose with a transient increase in $[Ca^{2+}]_{IC}$ followed by fast calcium oscillations on a sustained plateau (**Figure 6C**, upper panel).

As all beta cells are coupled into a single, large, functional syncytium, these oscillations are also very well synchronized among different cells by means of spreading $[Ca^{2+}]_{IC}$ waves[32,34,52-54] (**Figure 7C**). Slower $[Ca^{2+}]_{IC}$ oscillations with a period of 5–15 minutes may underlie the fast oscillations or even be the predominant type of reponse[55,56]. The same simple protocol may reveal other types of responses, especially at the periphery of islets (**Figure 6C**, lower panel). As these cells are not synchronized with beta cells and respond with faster and more irregular oscillations that are already present in low glucose conditions or with a decrease in activity, such responses are highly suggestive of non-beta cells[21,32,57-58]. However, their definitive functional characterization requires more complex protocols with additional stimulation steps or alternative approaches, which are discussed below. Typical responses of acinar and ductal cells are presented in **Figure 6D** and **Figure 6E**, respectively. Refer to the literature for more details on acinar and ductal cells[22,23,35].

Insert **Figure 6 here.**

After successful calcium imaging, the data are first exported and corrected for bleaching by a combination of an exponential and linear fit, as described in the protocol section. A time series before and after bleaching correction is presented in **Figure 7A**. Thereafter, several parameters in the activation and deactivation phase of the response as well as the plateau phase can be analyzed. A delay in the onset of $[Ca^{2+}]_{IC}$ increase after stimulation can be measured as represented by $delay_A$ in **Figure 7B** and the heterogeneity in delays among individual cells ($delay_{A1}$). The same parameters ($delay_D$ and $delay_{D1}$) can be used to describe the deactivation phase. Following the initial transient $[Ca^{2+}]_{IC}$ increase, the plateau phase in most pancreatic beta cells in an islet is characterized by relatively regular high frequency $[Ca^{2+}]_{IC}$ oscillations. The plateau phase can be described by analyzing the classical functional parameters. The schematic presentation of $[Ca^{2+}]_{IC}$ oscillations duration, frequency, and percentage of active time are presented in **Figure 7C**. In calcium imaging with acquisition rates higher than 10 Hz, calcium waves repeatedly spreading across the islet can also be recognized clearly (**Figure 7C**).

Insert **Figure 7 here.**

FIGURE AND TABLE LEGENDS:

Figure 1: Workflow diagram. Schematic representation of all steps in the process of pancreatic

tissue slice preparation, beginning with the injection of agarose into the common bile duct, followed by extraction of the pancreas and slicing. The prepared slices can be used for assessing the viability of the tissue with a Live/Dead kit or stained with a calcium sensor. Once stained, they are ready for imaging. Recordings obtained from the imaging process are then used for data analysis.

Figure 2: Injection of agarose into the common bile duct. (**A**) Open the abdominal cavity, and expose the organs in the peritoneal cavity. (**B**) The magnified part of the area enclosed by the rectangle in panel **A**. The white spot on the duodenum (indicated by the arrow) indicates the ampulla of Vater. Islets of Langerhans are denoted by arrowheads. (**C**) Clamp the ampulla of Vater by a curved hemostat, and raise it slightly to expose and gently stretch the common bile duct (arrow). (**D**) Cannulation of the common bile duct and the injection of 1.9% agarose solution using a 5 mL syringe and a 30 G needle.

Figure 3: Pancreas tissue preparation and slicing. (**A**) The extracted mouse pancreas after agarose injection. White tissue on the left indicates a well-injected part (duodenal part), while the more reddish part on the right shows the insufficiently injected part of the pancreas (splenic part). (**B**) Vibratome slicing of two blocks of pancreas tissue embedded in agarose. (**C**) Acute pancreatic tissue slice with islets of Langerhans indicated by arrowheads. Scale bar = 3000 µm. (**D**) Acute pancreatic tissue slice under the light microscope with the islet of Langerhans indicated by an arrowhead, asterisk indicates a pancreatic duct. Scale bar = 100 µm.

Figure 4: Viability of cells within the tissue slice. Viability of cells was determined with the Live/Dead assay. Live cells are stained by Calcein AM (shown in green), while dead cells are stained with ethidium homodimer-1 (shown in red). Yellow lines denote the position of the X-Y cross section of the Z-stack displayed at the bottom and the right. The full depth of the Z-stack is 88 µm.

Figure 5: Examples of usable and unusable preparations. (**A**) An example of a successful preparation of the pancreas tissue slice with well-stained cells in the islets of Langerhans, as well as ductal cells and surrounding acinar tissue. (**B**) An example of a poorly stained tissue slice. (**C**) Example of an islet of Langerhans with structural discontinuations. (**D**) An example of an islet of Langerhans containing many dead cells and a lot of debris. The “glow-over, glow-under” lookup table on the right displays 0 intensity in green and saturation in blue. Scale bar = 100 µm.

Figure 6: Representative results of calcium dynamics in distinct types of pancreatic cells. (**A**) A high-resolution image of an islet of Langerhans with surrounding tissue. Scale bar = 100 µm. (**B**) Delineation of distinct parts of pancreatic tissue with acinar tissue shown in yellow, an islet of Langerhans shown in red, and a segment of the ductal tree in blue. Scale bar = 100 µm. (**C**) Typical traces of calcium dynamics in beta and putative non-beta cells during stimulation with 12 mM glucose; 3 mM glucose was used for non-stimulatory conditions. Protocols that can be used for more specific discrimination of non-beta cells are described in the discussion section. (**D**) A typical trace of calcium dynamics of acinar cells stimulated by 25 nM acetylcholine. (**E**) A typical trace of calcium dynamics of ductal cells stimulated by 1 mM chenodeoxycholic acid.

Figure 7: Analysis of time-series data. (**A**) Correction of time-series data for photobleaching. (**B**) Analysis of delays to activation after stimulation and to deactivation after cessation of stimulation with 12 mM glucose. Duration of stimulation is denoted by the light gray, shaded bar in the image. (**C**) Analysis of several parameters of the plateau phase: I) Duration of the oscillation determined at half-height, II) frequency of oscillations determined by inter-oscillation intervals. III) active time as a product of frequency and duration of oscillations. I–IV) Delays between oscillations in any given wave of oscillations that spread across the islet of Langerhans determined by the delays (Δt) in time at which a single cell reaches half-height of the oscillation.

DISCUSSION:

The pancreatic tissue slice method is a fast experimental method to study the morphology and physiology of the endocrine and exocrine parts of the pancreas in a more conserved, in situ preparation. Many of the advantages have already been pointed out in the Introduction. It is worth pointing out that in general (i.e., not only for calcium imaging), the slice approach to study pancreatic physiology saves time because it does not involve a recovery period after isolation. The latter is not absolutely necessary with all types of experiments and uses of isolated islets from different species, but is typically employed to increase purity, restore viability and functionality, and sometimes to collect islets from several donors[59-64]. However, in the context of calcium imaging, beta cell responses have been found to depend on culture duration and conditions, and this is an important source of variation that should be taken into account when using isolated islets[15,65]. The same issue should be considered for tissue slices if their long-term culture becomes a widely used option in the future[22,36]. The tissue slice method also has a high yield and thus potentially reduces animal suffering and increases statistical power. Moreover, as many slices can be prepared from a single animal and because the slices survive for long periods, including the same animal or even the same islet in both the experimental and the control groups becomes feasible.

As the original architecture and cell-to-cell communications are preserved, and because it is compatible with a number of structural analyses, electrophysiological, imaging methods, and hormone secretion assays, this method is especially useful to study pancreatic functions that depend on undisturbed interactions between individual cells, e.g., sensitivity to secretagogues, paracrine and immune interactions between different cell types, patterns of electrical activity, properties of calcium dynamics, and the secretion of different hormones. For calcium imaging specifically, the main advantages of using slices are the exposure of the islet core and the possibility to acquire signals from many different cell types with high resolution. Depending on the requirements of the experiment and the age of animals, the thickness can be varied, the slices can be transfected, or obtained from animals with genetically encoded reporters. As explained in more detail below, the latter two approaches also enable specific functional identification and characterization of responses from non-beta cells [31,66]. Moreover, islets from well-defined parts of the organ can be studied for differences in responsiveness or susceptibility to disease. Although they do not require a recovery incubation period, they can easily be incubated with different pharmacological agents, fatty acids, high glucose, and cytokines.

Most importantly, as high resolution is achievable in combination with single-cell or even subcellular resolution, confocal calcium imaging in slices is one of the most suitable methods for analyzing calcium waves, functional connectivity, and the different functional roles of cells in distinct parts of an islet[54,67]. Despite a number of advantages, the tissue slice approach has important limitations. First, it is still at least partly disruptive to islet and exocrine architecture, especially at the cut surface, and precautions, such as low temperature, frequent exchange of solutions, and gentle and quick manipulation, are needed during preparation to prevent additional mechanical and endogenous enzymatic damage. Second, the patterns of nutrient and secretagogue delivery are still inferior to the in vivo route, the preparation is detached from systemic innervation, and inter-organ feedback, such as between the islet and its target tissues, is impossible, in contrast to in vivo approaches. Third, maximum slice thickness is limited by oxygenation, nutrient delivery, and pH regulation at ~200 µm[9]. Further, both preparation of slices and imaging need a lot of training, and in-depth analyses of calcium data from long time series and from many cells require specialized knowledge that is often not included in the toolkit of a classical physiologist and requires help from physicists or data scientists. The advantage that homo- and heterotypic interactions are preserved can also complicate the analysis of samples due to the presence of signals from other cells in regions of interest. Depending on protocols, activation of other cells can lead to indirect additional stimulation or inhibition of an observed cell.

This can only be resolved conclusively by deconvolution approaches, by more complex stimulation protocols including substances that block some of the indirect effects, by using specific knock-out animals, and by careful comparison of results with results from other studies employing more reductionist methodologies. Additionally, if secretion measurements are necessary, it should be kept in mind that some slices may lack islets, and the total mass of endocrine tissue in a single slice is typically low. The preparation of acute pancreatic tissue slices for imaging involves several critical steps discussed in the following sections and summarized in **Table 1**, where the reader can also find short, but important tips for troubleshooting. First, when preparing the agarose solution, the agarose powder must dissolve completely, otherwise the undissolved particles may obstruct the injection. Keep the homogeneous agarose solution at 37–45 °C to prevent hardening of agarose due to too low a temperature on the one hand and to prevent tissue damage due to too high temperatures on the other hand. After use, the remaining agarose may be stored at 4 °C and reheated, although repeated reheating can result in increased density due to water evaporation, eventually making the injection difficult or impossible.

The next critical step in the preparation is clamping the major duodenal papilla correctly. A white spot on the duodenum indicates the junction of the common bile duct and the duodenum. A clamp placed too proximally will result in obstruction of some lateral pancreatic branches of the common duct, disabling the injection of these parts, whereas a clamp placed too distally will result in agarose leaking through the lower resistance path directly into the duodenum. Before cannulation of the common bile duct, the surrounding adipose tissue can be carefully removed for better visualization of the duct and greater control during injection. Insufficient precision during removal of the surrounding tissue may result in perforation of the duct. The selection of the needle diameter used for agarose injection is also important. In mice, a 30 G needle is

preferably used; smaller (32 or 33 G) needles require more effort due to high viscosity of the agarose solution and are more prone to obstruction. However, if used in combination with a lower-density agarose solution, they can be very helpful in smaller mouse strains and younger animals. During the initial postnatal days, agarose may alternatively be injected subcapsularly rather than intraductally[2]. Using needles with greater diameter in mice will most probably result in damaging the common bile duct. This can also happen with the correct needle diameter, and a forceps can help in keeping the needle in place during injection. Larger diameter needles may be the only solution in case of larger ducts, as found in rats. If the needle is too narrow to ensure a tight seal preventing back-leakage, a ligature may be placed around it upon successful entry into the duct.

Agarose injection takes some effort due to the solution's viscosity, and once the injection process has started, it should not be interrupted as the low-melting-point agarose solution may solidify in the needle or the largest parts of the ductal tree before the injection is completed. This will result in poor tissue penetration and worse support during cutting. The duct should always be cannulated at the point where the left hepatic duct and the cystic duct join to form the common bile duct.. If the common bile duct gets perforated, repeatedly try cannulating closer to the duodenum. When the pancreas is sufficiently stabilized with agarose solution and extracted from the peritoneal cavity, small pieces of well-injected tissue are cut. Before embedding them into the agarose, it is crucial to remove all the adipose and connective tissues as their residues make slicing more challenging. The same applies to blood vessels and duct residues, except when they are the focus of the experiment. In this case, make sure to position them in such a way that the desired cross-section will be obtained. When embedding the tissue in agarose, ensure that the temperature is appropriate (37 °C), and that the tissue is completely surrounded by agarose, as forces during vibratome slicing can rip out the pancreas tissue from the agarose blocks.

Quickly drying the tissue blocks before placing them in agarose by placing them briefly on a paper tissue can help prevent poor contact between tissue and agarose during this step. During solidification of agarose blocks, place the Petri dish horizontally, and prevent contact between the pancreas tissue and the bottom of the Petri dish. If the pancreas is not fully injected, the cutting process will be challenging. Therefore, try to reduce the cutting speed to obtain tissue slices. To minimize cell damage during vibratome slicing, replace the ECS (and the ice cubes made of ECS) in the slicing chamber regularly. The latter will reduce the activity of pancreatic enzymes released from acinar tissue during slicing. The thickness of the slices is also of crucial importance. For calcium dynamics and electrophysiological experiments, 140 µm slices are usually cut; however, according to the aim of the study, slice thickness can range from 90 µm to 200 µm. Keep in mind that in thicker slices, the diffusion of oxygen and nutrients will be limited, but they will include more tissue. Additionally, the proportion of uncut islets may be expected to increase with increasing slice thickness. Slices can be stored in a regularly exchanged ECS at room temperature for several hours or even cultivated in an appropriate cell medium for several days; however, this may eventually affect the normal islet cell physiology[3,22].

When preparing the dye solution, ensure careful mixing of all components, and avoid exposure to ambient light. The pancreatic slice is composed of many cell layers, and the uptake of calcium

dye is limited to the first few most superficial cell layers, as described previously for isolated islets[58,68], and pituitary slices[69]. However, in contrast to isolated islets where the surrounding capsule and outer cell layers hinder the penetration of the dye into deeper layers, tissue slices permit access to the entire cross-sectional surface of the islet, enabling simultaneous measurement of calcium dynamics in hundreds of cells from all layers of an islet. Fluorescent Ca^{2+} indicators are the most widely used for measuring calcium dynamics, and together with CLSM, they enable recordings with high temporal resolution, reaching several hundred Hertz. When selecting the most appropriate fluorescent Ca^{2+} indicator, consider different factors, including the indicator form, which influences the cell loading method, measurement mode (qualitative or quantitative), and dissociation constant (K_d) that needs to be in the Ca^{2+} concentration range of interest and depends on pH, temperature, presence of Mg^{2+} and other ions, as well as protein binding. As cellular Ca^{2+} signals are usually transient, the Ca^{2+} binding rate constant should also be considered. For measuring $[Ca^{2+}]_{IC}$ dynamics in pancreatic cells, this group mainly uses the cell-permeable Ca2+ indicator dye described in this protocol (**Table of Materials**) as it is a long wavelength indicator with the emission wavelengths in the spectrum where cellular autofluorescence is usually less problematic, and the energy of excitation light is low, which reduces the potential for cellular photodamage. Because this dye is fluorescent at low Ca^{2+} concentrations, this facilitates the determination of baseline $[Ca^{2+}]_{IC}$ and increases cellular visibility before stimulation. After binding Ca^{2+}, the fluorescence intensity of the dye increases 14-fold, enabling detection of even slight changes in $[Ca^{2+}]_{IC}$.

For successful live-cell calcium imaging, several crucial hardware parameters need to be considered, as described in the protocol section. For live-cell imaging wherein signal amplitudes are low and chances of phototoxicity are high, objectives with a higher NA are preferably used to collect more light from the specimen. If calcium dynamics must be recorded with a high temporal resolution, use the resonant scanner instead of linear galvanometers. Besides choosing the right objective, the use of highly sensitive detectors—such as hybrid detectors that require less laser power—avoids phototoxicity and photobleaching. This is of special importance for long-lasting calcium imaging. Other important steps in calcium imaging are parameter settings of image quality for time series acquisitions. The most important are the temporal and the spatial resolution. As the calcium dynamics per se determines the lowest acceptable temporal resolution, the sampling rate needs to be at least two-fold higher than the expected signal frequency to detect the signal or even 10 times higher to detect the shape of the signal reliably. In acute pancreatic tissue slices, calcium dynamics can be measured in hundreds of cells simultaneously and therefore, the spatial resolution is also important. This can be enhanced by increasing the number of pixels or by increasing the line averaging during live acquisition. However, because of the inverse relationship between the spatial and the temporal resolution, a trade-off between both settings is needed.

If calcium imaging has to be performed in a specific cell population within the pancreas, a stimulus able to functionally differentiate the cells within the slice is necessary. High glucose reliably and quickly activates beta cells to an oscillatory pattern that is superimposed on an elevated calcium level and is highly synchronized among all cells within an islet[32,58,70]. The beta cells are the most numerous cell type within an islet and are located mostly in the islet core in

mice. The same stimulation protocol decreases and sometimes does not appreciably change the bursting in alpha cells[30,32,58,70-72]. To discriminate alpha cells functionally, low (3 mM) glucose, glutamate or adrenalin can be used to increase their frequency or basal $[Ca^{2+}]_{IC}$[21,72-75]. They represent 10–20% of islet cells and will be detected on the islet periphery[1]. Delta cells are also found on the periphery. They make up only ~5% of the total number of endocrine cells in an islet and are typically active in 6 mM glucose and respond to glucose stimulation with an increased irregular bursting activity from the baseline or a slightly elevated calcium level[1,32,71,76]. Ghrelin can be used for specific stimulation of delta cells[21,77-79] in calcium imaging experiments. However, protocols for specific functional identification of PP and epsilon cells remain to be defined. Further, 25 nM acetylcholine reliably activates acinar cells into bursting activity[35,80,81]. Additionally, a number of other secretagogues, such as cerulein, cholecystokinin, and carbamylcholine, can be used to evoke calcium responses in acinar cells[22,40,82,83].

Finally, 1 mM chenodeoxycholic acid reliably evokes calcium responses in ductal cells in tissue slices; angiotensin II, ATP, and some other secretagogues can also be used[11,23,84,85]. Whenever a functional identification based on characteristic responses to specific secretagogues and inhibitors is not sufficient, genetically labelled animals[31], transfected cells[73], or immunocytochemistry can be employed for the identification of different cell types[9,22,71,86]. During the last couple of years, the tissue slice method has been successfully adapted to human tissue, opening many new important research avenues in both exocrine[41] and endocrine physiology[9,36,37,39]. Interestingly, a detailed assessment of calcium dynamics in human islets has been notoriously difficult and remains to be investigated in greater detail[87]. Combined with advanced confocal microscopy, the pancreatic tissue slice method has enabled many new insights into the calcium dynamics in mice and will hopefully do the same for human tissue.

ACKNOWLEDGMENTS:

The work presented in this study was financially supported by the Slovenian Research Agency (research core funding nos. P3-0396 and I0-0029, as well as research projects nos. J3-9289, N3-0048, and N3-0133) and by the Austrian Science Fund / Fonds zur Förderung der Wissenschaftlichen Forschung (bilateral grants I3562--B27 and I4319--B30). We thank Maruša Rošer, Maša Čater, and Rudi Mlakar for excellent technical assistance.

DISCLOSURES:

The authors declare that the research was conducted in the absence of any commercial or financial interest.

REFERENCES:

1 Dolensek, J., Rupnik, M. S., Stozer, A. Structural similarities and differences between the human and the mouse pancreas. *Islets.* **7** (1), e1024405 (2015).

2 Meneghel-Rozzo, T., Rozzo, A., Poppi, L., Rupnik, M. In vivo and in vitro development of mouse pancreatic ß-cells in organotypic slices. *Cell and Tissue Research.* **316** (3), 295–303 (2004).

3 Rozzo, A., Meneghel-Rozzo, T., Delakorda, S. L., Yang, S. B., Rupnik, M. Exocytosis of insulin: in vivo maturation of mouse endocrine pancreas. *Annals of the New York Academy of the Sciences.* **1152**, 53–62 (2009).

4 Dolenšek, J., Pohorec, V., Rupnik, M. S., Stožer, A. Pancreas physiology, challenges in pancreatic pathology. Seicean. A. (Ed) *IntechOpen*, doi: 10.5772/65895 (2017).
5 Williams, J. A. The nobel pancreas: a historical perspective. *Gastroenterology.* **144** (6), 1166–1169 (2013).
6 Lacy, P. E., Kostianovsky, M. Method for the isolation of intact islets of Langerhans from the rat pancreas. *Diabetes.* **16** (1), 35–39 (1967).
7 Williams, J. A., Korc, M., Dormer, R. L. Action of secretagogues on a new preparation of functionally intact, isolated pancreatic acini. *American Journal of Physiology.* **235** (5), 517–524 (1978).
8 Peikin, S. R., Rottman, A. J., Batzri, S., Gardner, J. D. Kinetics of amylase release by dispersed acini prepared from guinea pig pancreas. *American Journal of Physiology.* **235** (6), E743–E749 (1978).
9 Marciniak, A. et al. Using pancreas tissue slices for in situ studies of islet of Langerhans and acinar cell biology. *Nature Protocols.* **9** (12), 2809–2822 (2014).
10 Skelin, M., Rupnik, M., Cencic, A. Pancreatic beta cell lines and their applications in diabetes mellitus research. *Altex-Alternatives to Animal Experimentation.* **27** (2), 105–113 (2010).
11 Molnar, R. et al. Mouse pancreatic ductal organoid culture as a relevant model to study exocrine pancreatic ion secretion. *Laboratory Investigation.* **100** (1), 84–97 (2020).
12 Rupnik, M. The physiology of rodent beta-cells in pancreas slices. *Acta Physiologica (Oxford, England).* **195** (1), 123–138 (2009).
13 Blinman, T. A. et al. Activation of pancreatic acinar cells on isolation from tissue: cytokine upregulation via p38 MAP kinase. *American Journal of Physiology. Cell Physiology.* **279** (6), C1993–2003 (2000).
14 Speier, S., Rupnik, M. A novel approach to in situ characterization of pancreatic ß-cells. *Pflügers Archive: European Journal of Physiology.* **446** (5), 553–558 (2003).
15 Gilon, P., Jonas, J., Henquin, J. Culture duration and conditions affect the oscillations of cytoplasmic calcium concentration induced by glucose in mouse pancreatic islets. *Diabetologia.* **37** (10), 1007–1014 (1994).
16 Huang, C., Gu, G. Effective isolation of functional islets from neonatal mouse pancreas. *Journal of Visualized Experiments: JoVE*. (119), 55160 (2017).
17 Szot, G. L., Koudria, P., Bluestone, J. A. Murine pancreatic islet isolation. *Journal of Visualized Experiments: JoVE.* (7), 255 (2007).
18 Qi, M. et al. Human pancreatic islet isolation: Part I: digestion and collection of pancreatic tissue. *Journal of Visualized Experiments: JoVE.* (27), 1125 (2009).
19 Qi, M. *et al.* Human pancreatic islet isolation: Part II: purification and culture of human islets. *Journal of Visualized Experiments: JoVE.* (27), 1343 (2009).
20 Stull, N. D., Breite A., McCarthy, R., Tersey, S. A., Mirmira, R. G. Mouse islet of Langerhans isolation using a combination of purified collagenase and neutral protease. *Journal of Visualized Experiments: JoVE.* (67), 4137 (2012).
21 Hamilton, A., Vergari, E., Miranda, C., Tarasov, A. I. Imaging calcium dynamics in subpopulations of mouse pancreatic islet cells. *Journal of Visualized Experiments: JoVE.* (153), doi: 10.3791/59491 (2019).
22 Marciniak, A., Selck, C., Friedrich, B., Speier, S. Mouse pancreas tissue slice culture facilitates long-term studies of exocrine and endocrine cell physiology in situ. *PLoS ONE.* **8** (11),

837 e78706–e78706 (2013).
838 23 Gal, E. et al. A Novel in situ approach to studying pancreatic ducts in mice. *Frontiers in*
839 *Physiology.* **10**, 938 (2019).
840 24 Speier, S., Yang, S. B., Sroka, K., Rose, T., Rupnik, M. KATP-channels in beta-cells in tissue
841 slices are directly modulated by millimolar ATP. *Molecular and Cellular Endocrinology.* **230** (1–2),
842 51–58 (2005).
843 25 Speier, S., Gjinovci, A., Charollais, A., Meda, P., Rupnik, M. Cx36-mediated coupling
844 reduces β-cell heterogeneity, confines the stimulating glucose concentration range, and affects
845 insulin release kinetics. *Diabetes.* **56** (4), 1078–1086 (2007).
846 26 Rose, T., Efendic, S., Rupnik, M. Ca2+-secretion coupling is impaired in diabetic Goto
847 Kakizaki rats. *The Journal of General Physiology.* **129** (6), 493–508 (2007).
848 27 Paulmann, N. et al. Intracellular serotonin modulates insulin secretion from pancreatic β-
849 cells by protein serotonylation. *PLoS Biology.* **7** (10), e1000229 (2009).
850 28 Mandic, S. A. et al. Munc18-1 and Munc18-2 proteins modulate β-cell Ca2+ sensitivity and
851 kinetics of insulin exocytosis differently. *Journal of Biological Chemistry.* **286** (32), 28026–28040
852 (2011).
853 29 Dolensek, J., Skelin, M., Rupnik, M. S. Calcium dependencies of regulated exocytosis in
854 different endocrine cells. *Physiological Research.* **60**, S29–S38 (2011).
855 30 Huang, Y.-C., Rupnik, M., Gaisano, H. Y. Unperturbed islet α-cell function examined in
856 mouse pancreas tissue slices. *Journal of Physiology.* **589** (2), 395–408 (2011).
857 31 Huang, Y.-C. et al. In situ electrophysiological examination of pancreatic α cells in the
858 streptozotocin-induced diabetes model, revealing the cellular basis of glucagon hypersecretion.
859 *Diabetes.* **62** (2), 519–530 (2013).
860 32 Stožer, A., Dolenšek, J., Rupnik, M. S. Glucose-stimulated calcium dynamics in islets of
861 Langerhans in acute mouse pancreas tissue slices. *PLoS ONE.* **8** (1), e54638 (2013).
862 33 Stožer, A. et al. Functional connectivity in islets of Langerhans from mouse pancreas tissue
863 slices. *PLoS Computational Biology.* **9** (2), e1002923 (2013).
864 34 Dolenšek, J., Stožer, A., Skelin Klemen, M., Miller, E. W., Slak Rupnik, M. The relationship
865 between membrane potential and calcium dynamics in glucose-stimulated beta cell syncytium in
866 acute mouse pancreas tissue slices. *PLoS ONE.* **8** (12), e82374 (2013).
867 35 Perc, M., Rupnik, M., Gosak, M., Marhl, M. Prevalence of stochasticity in experimentally
868 observed responses of pancreatic acinar cells to acetylcholine. *Chaos.* **19** (3), 037113 (2009).
869 36 Qadir, M. M. F. et al. Long-term culture of human pancreatic slices as a model to study
870 real-time islet regeneration. *Nature Communications.* **11** (1), 3265–3265 (2020).
871 37 Panzer, J. K. et al. Pancreas tissue slices from organ donors enable in situ analysis of type
872 1 diabetes pathogenesis. *JCI Insight.* **5** (8), e134525 (2020).
873 38 Cohrs, C. M. et al. Vessel network architecture of adult human islets promotes distinct
874 cell-cell interactions in situ and is altered after transplantation. *Endocrinology.* **158** (5), 1373–
875 1385 (2017).
876 39 Cohrs, C. M. et al. Dysfunction of persisting beta cells is a key feature of early type 2
877 diabetes pathogenesis. *Cell Reports.* **31** (1), 107469 (2020).
878 40 Dolai, S. et al. Pancreatitis-induced depletion of syntaxin 2 promotes autophagy and
879 increases basolateral exocytosis. *Gastroenterology.* **154** (6), 1805–1821 e1805 (2018).
880 41 Liang, T. et al. Ex vivo human pancreatic slice preparations offer a valuable model for

studying pancreatic exocrine biology. *Journal of Biological Chemistry.* **292** (14), 5957–5969 (2017).
42 Panzer, J. K., Cohrs, C. M., Speier, S. Using pancreas tissue slices for the study of islet physiology. *Methods in Molecular Biology.* **2128,** 301–312 (2020).
43 Klemen, M., Dolenšek, J., Stožer, A., Rupnik, M. in *Exocytosis Methods*. Thorn, P. (Ed) Chapter 7, 127–146, Humana Press (2014).
44 Speier, S. Experimental approaches for high-resolution in vivo imaging of islet of Langerhans biology. *Current Diabetes Reports.* **11** (5), 420–425 (2011).
45 Leibiger, I. B., Berggren, P.-O. Intraocular in vivo imaging of pancreatic islet cell physiology/pathology. *Molecular Metabolism.* **6** (9), 1002–1009 (2017).
46 Reissaus, C. A. et al. A Versatile, portable intravital microscopy platform for studying beta-cell biology in vivo. *Scientific Reports.* **9** (1), 8449 (2019).
47 Jacob, S. et al. In vivo Ca(2+) dynamics in single pancreatic beta cells. *FASEB Journal.* **34** (1), 945–959 (2020).
48 Fernandez, J., Valdeolmillos, M. Synchronous glucose-dependent [Ca2+]i oscillations in mouse pancreatic islets of Langerhans recorded in vivo. *FEBS Letters.* **477** (1–2), 33–36 (2000).
49 Almaca, J., Weitz, J., Rodriguez-Diaz, R., Pereira, E., Caicedo, A. The pericyte of the pancreatic islet regulates capillary diameter and local blood flow. *Cell Metabolism.* **27** (3), 630–644 e634 (2018).
50 Weitz, J. R. et al. Mouse pancreatic islet macrophages use locally released ATP to monitor beta cell activity. *Diabetologia.* **61** (1), 182–192 (2018).
51 Tian, G., Sandler, S., Gylfe, E., Tengholm, A. Glucose- and hormone-induced cAMP oscillations in α- and β-cells within intact pancreatic islets. *Diabetes.* **60** (5), 1535–1543 (2011).
52 Benninger, R. K., Zhang, M., Head, W. S., Satin, L. S., Piston, D. W. Gap junction coupling and calcium waves in the pancreatic islet. *Biophysical Journal.* **95** (11), 5048–5061 (2008).
53 Santos, R. M. et al. Widespread synchronous Ca oscillations due to bursting electrical activity in single pancreatic islets. *Pflügers Archive: European Journal of Physiology.* **418** (4), 417–422 (1991).
54 Šterk, M. et al. Assessing the origin and velocity of Ca2+ waves in three-dimensional tissue: Insights from a mathematical model and confocal imaging in mouse pancreas tissue slices. *Communications in Nonlinear Science and Numerical Simulation.* **93**, 105495 (2021).
55 Gosak, M. et al. Critical and supercritical spatiotemporal calcium dynamics in beta cells. *Frontiers in Physiology.* **8**, 1106 (2017).
56 Satin, L. S., Butler, P. C., Ha, J., Sherman, A. S. Pulsatile insulin secretion, impaired glucose tolerance and type 2 diabetes. *Molecular Aspects in Medicine.* **42**, 61–77 (2015).
57 Tengholm, A., Gylfe, E. Oscillatory control of insulin secretion. *Molecular and Cellular Endocrinology.* **297** (1–2), 58–72 (2009).
58 Quesada, I. et al. Glucose induces opposite intracellular Ca^{2+} concentration oscillatory patterns in identified α- and β-cells within intact human islets of Langerhans. *Diabetes.* **55** (9), 2463–2469 (2006).
59 Ferguson, J., Allsopp, R. H., Taylor, R. M. & Johnston, I. D. Isolation and long term preservation of pancreatic islets from mouse, rat and guinea pig. *Diabetologia.* **12** (2), 115–121 (1976).
60 Andersson, A. Isolated mouse pancreatic islets in culture: effects of serum and different

culture media on the insulin production of the islets. *Diabetologia.* **14** (6), 397–404 (1978).
61 Ramirez-Dominguez, M. Isolation of mouse pancreatic islets of Langerhans. *Advances in Experimental Medicine and Biology.* **938**, 25–34 (2016).
62 Carter, J., Dula, S., Corbin, K., Wu, R., Nunemaker, C. A practical guide to rodent islet isolation and assessment. *Biological Procedures Online.* **11** (1), 3–31 (2009).
63 Daoud, J., Rosenberg, L., Tabrizian, M. Pancreatic islet culture and preservation strategies: advances, challenges, and future outlook. *Cell Transplantation.* **19** (12), 1523–1535 (2010).
64 Zawalich, W. S., Yamazaki, H., Zawalich, K. C. Biphasic insulin secretion from freshly isolated or cultured, perifused rodent islets: comparative studies with rats and mice. *Metabolism.* **57** (1), 30–39 (2008).
65 Roe, M. W. et al. Absence of effect of culture duration on glucose-activated alterations in intracellular calcium concentration in mouse pancreatic islets. *Diabetologia*. **38**, 876–877 (1995).
66 Shuai, H., Xu, Y., Yu, Q., Gylfe, E., Tengholm, A. Fluorescent protein vectors for pancreatic islet cell identification in live-cell imaging. *Pflügers Archive: European Journal of Physiology.* **468** (10), 1765–1777 (2016).
67 Dolenšek, J. et al. Glucose-dependent activation, activity, and deactivation of beta cell networks in acute mouse pancreas tissue slices. *bioRxiv.* doi: 10.1101/2020.03.11.986893 (2020).
68 Zhang, Q. et al. Cell coupling in mouse pancreatic beta-cells measured in intact islets of Langerhans. *Philosophical Transactions. Series A, Mathematical, Physical, and Engineering Sciences.* **366** (1880), 3503–3523 (2008).
69 Sánchez-Cárdenas, C., Hernández-Cruz, A. GnRH-induced Ca^{2+}-signalling patterns in mouse gonadotrophs recorded from acute pituitary slices in vitro. *Neuroendocrinology.* **91** (3), 239–255 (2010).
70 Asada, N., Shibuya, I., Iwanaga, T., Niwa, K., Kanno, T. Identification of alpha- and beta-cells in intact isolated islets of Langerhans by their characteristic cytoplasmic Ca^{2+} concentration dynamics and immunocytochemical staining. *Diabetes.* **47** (5), 751–757 (1998).
71 Nadal, A., Quesada, I., Soria, B. Homologous and heterologous asynchronicity between identified α-, β- and δ-cells within intact islets of Langerhans in the mouse. *Journal of Physiology.* **517** (1), 85–93 (1999).
72 Shuai, H., Xu, Y., Yu, Q., Gylfe, E., Tengholm, A. Fluorescent protein vectors for pancreatic islet cell identification in live-cell imaging. *Pflugers Archive: European Journal of Physiology.* **468** (10), 1765–1777 (2016).
73 Cabrera, O. et al. Glutamate is a positive autocrine signal for glucagon release. *Cell Metabolism*. **7** (6), 545–554 (2008).
74 Li, J. et al. Submembrane ATP and Ca2+ kinetics in α-cells: unexpected signaling for glucagon secretion. *FASEB Journal.* **29** (8), 3379–3388 (2015).
75 Hamilton, A. et al. Adrenaline stimulates glucagon secretion by Tpc2-dependent Ca(2+) mobilization from acidic stores in pancreatic α-cells. *Diabetes*. **67** (6), 1128–1139 (2018).
76 Arrojo, E. D. R. et al. Structural basis for delta cell paracrine regulation in pancreatic islets. *Nature Communications.* **10** (1), 3700 (2019).
77 DiGruccio, M. R. et al. Comprehensive alpha, beta and delta cell transcriptomes reveal that ghrelin selectively activates delta cells and promotes somatostatin release from pancreatic islets. *Molecular Metabolism.* **5** (7), 449–458 (2016).
78 Adriaenssens, A. E. et al. Transcriptomic profiling of pancreatic alpha, beta and delta cell

populations identifies delta cells as a principal target for ghrelin in mouse islets. *Diabetologia.* **59** (10), 2156–2165 (2016).
79 Rorsman, P., Huising, M. O. The somatostatin-secreting pancreatic δ-cell in health and disease. *Nature reviews. Endocrinology.* **14** (7), 404–414 (2018).
80 Petersen, C. C., Toescu, E. C., Petersen, O. H. Different patterns of receptor-activated cytoplasmic Ca2+ oscillations in single pancreatic acinar cells: dependence on receptor type, agonist concentration and intracellular Ca2+ buffering. *The EMBO journal.* **10** (3), 527–533 (1991).
81 Thorn, P., Lawrie, A. M., Smith, P. M., Gallacher, D. V., Petersen, O. H. Local and global cytosolic Ca2+ oscillations in exocrine cells evoked by agonists and inositol trisphosphate. *Cell.* **74** (4), 661–668 (1993).
82 Behrendorff, N., Floetenmeyer, M., Schwiening, C., Thorn, P. Protons released during pancreatic acinar cell secretion acidify the lumen and contribute to pancreatitis in mice. *Gastroenterology.* **139** (5), 1711–1720, 1720.e1711-1715 (2010).
83 Criddle, D. N. et al. Cholecystokinin-58 and cholecystokinin-8 exhibit similar actions on calcium signaling, zymogen secretion, and cell fate in murine pancreatic acinar cells. *American Journal of Physiology. Gastrointestinal and Liver Physiology.* **297** (6), G1085–1092 (2009).
84 Venglovecz, V. et al. Effects of bile acids on pancreatic ductal bicarbonate secretion in guinea pig. *Gut.* **57** (8), 1468–3288 (2008).
85 Maleth, J., Hegyi, P. Calcium signaling in pancreatic ductal epithelial cells: an old friend and a nasty enemy. *Cell Calcium.* **55** (6), 337–345 (2014).
86 Nadal, A., Quesada, I., Soria, B. Homologous and heterologous asynchronicity between identified alpha-, beta- and delta-cells within intact islets of Langerhans in the mouse. *Journal of Physiology.* **517** (Pt 1), 85–93 (1999).
87 Skelin Klemen, M., Dolenšek, J., Slak Rupnik, M., Stožer, A. The triggering pathway to insulin secretion: Functional similarities and differences between the human and the mouse β cells and their translational relevance. *Islets.* **9** (6), 109–139 (2017).

Figure 1

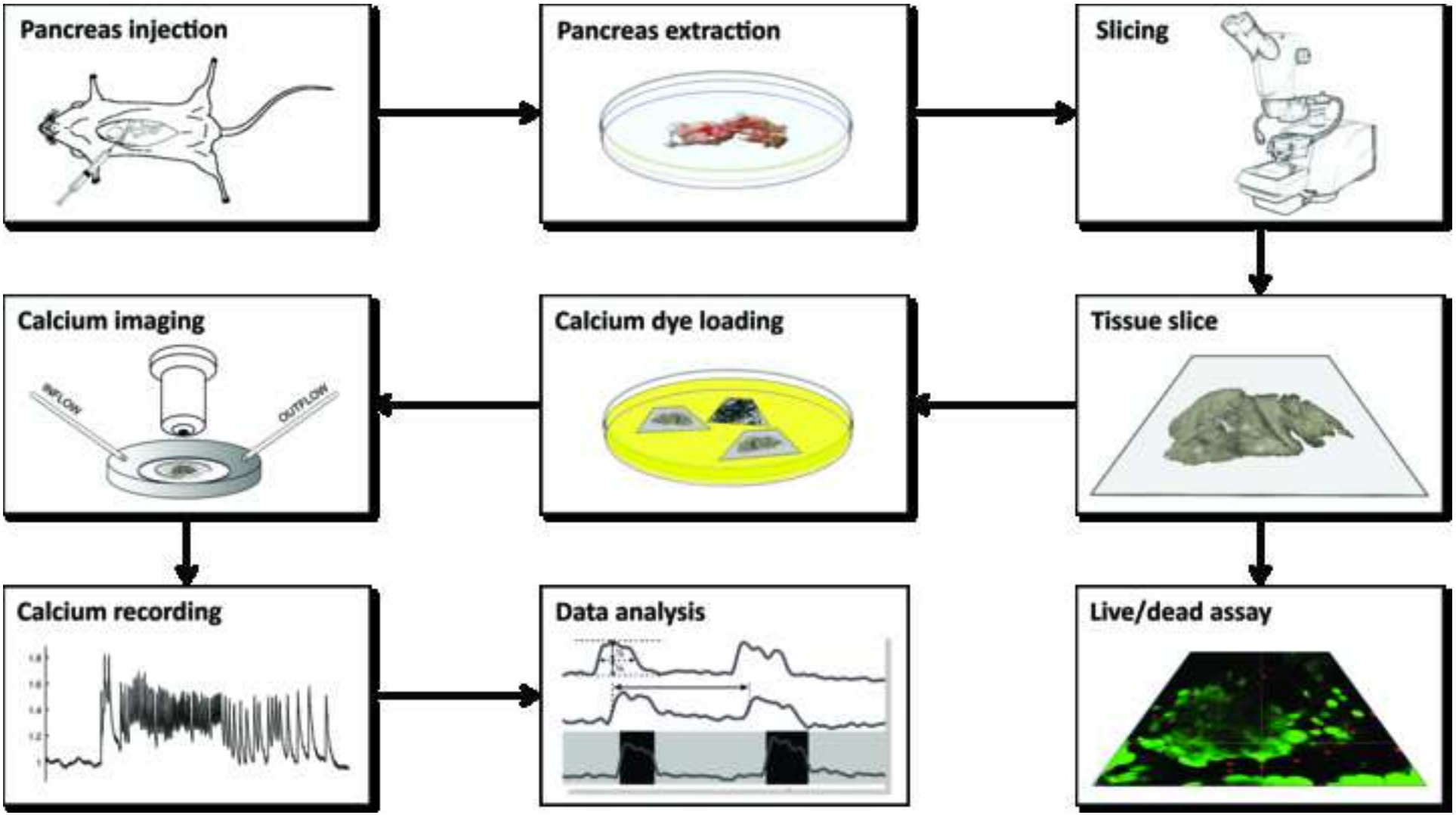

Figure 2

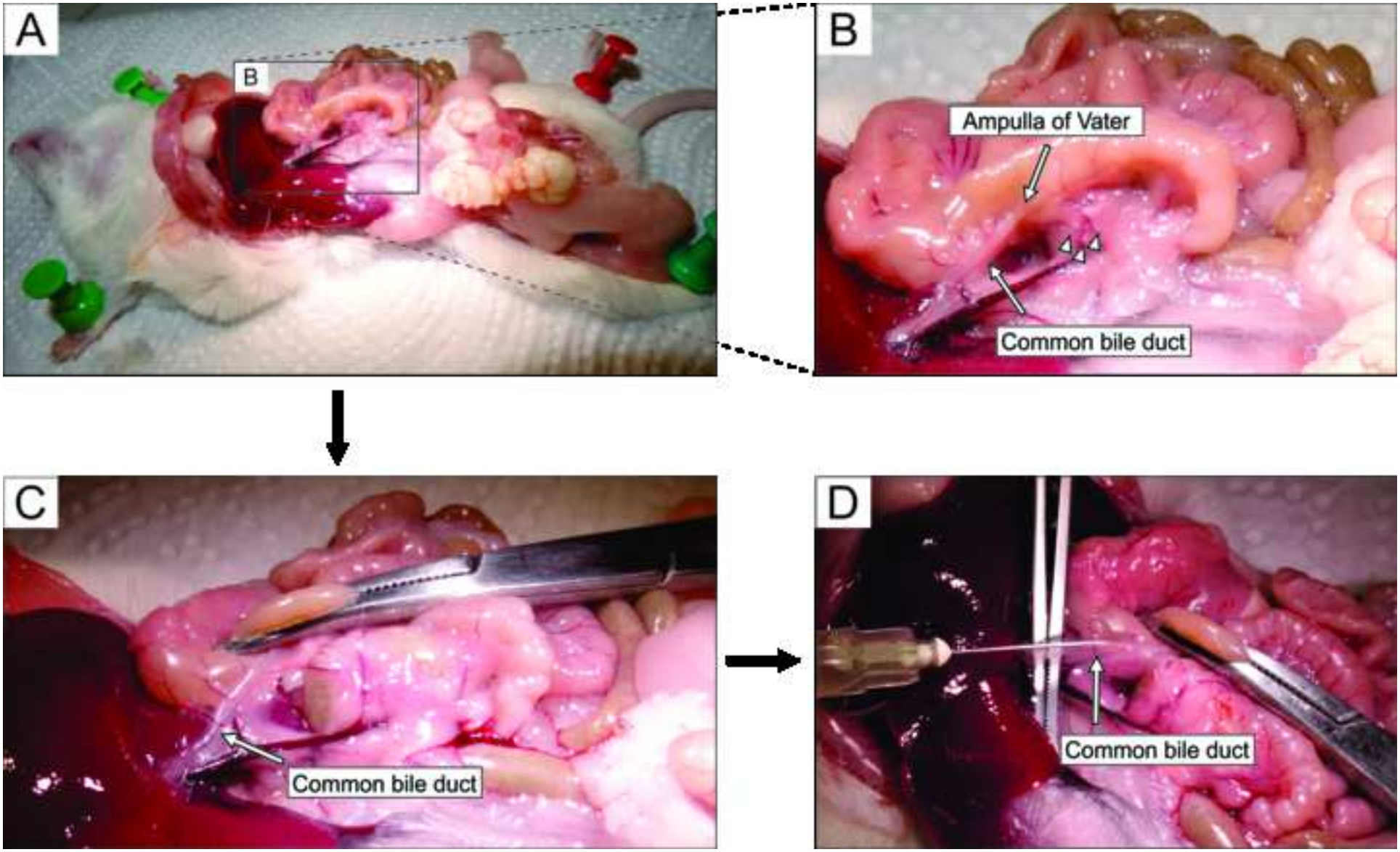

Figure 3

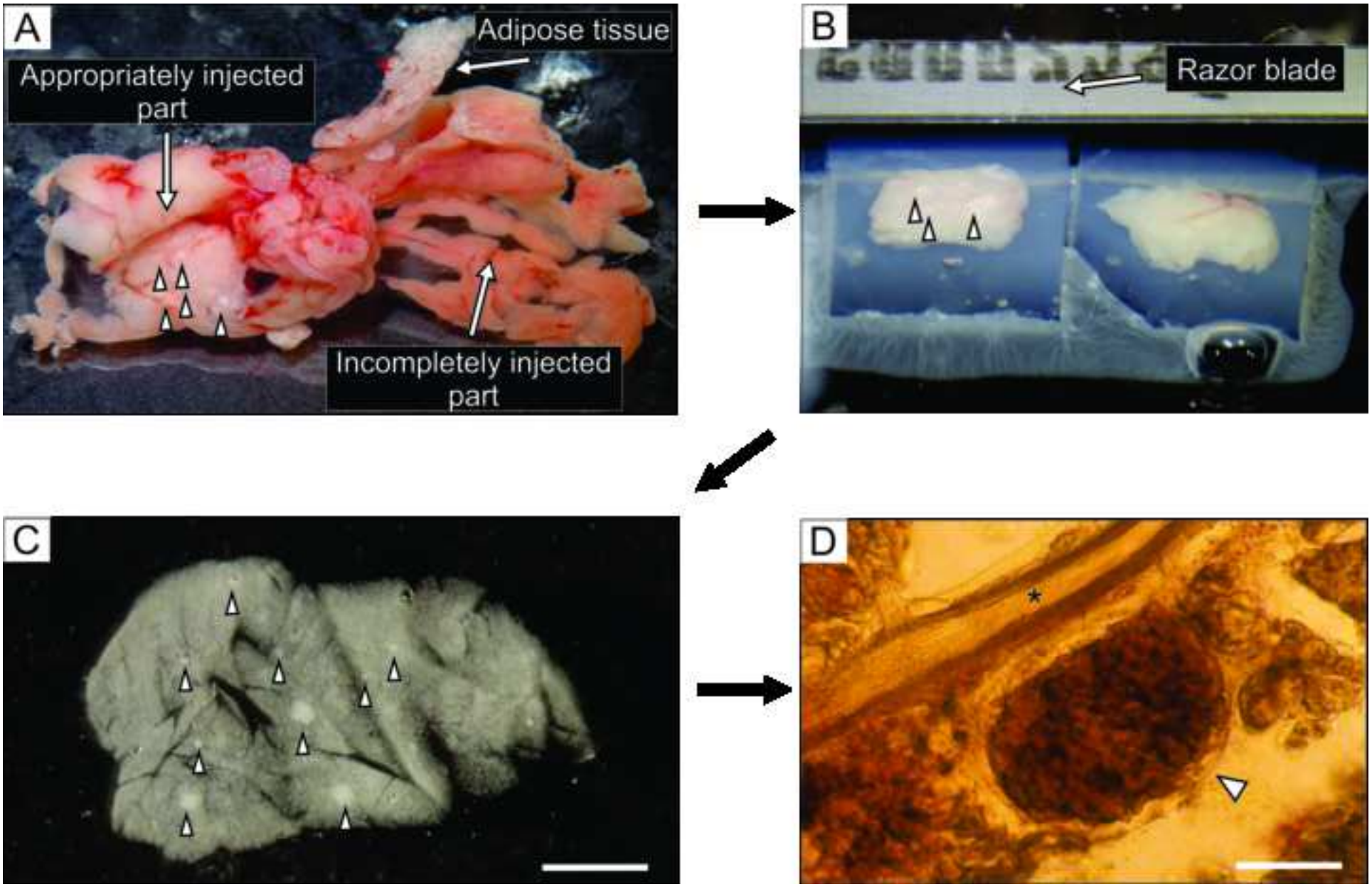

Figure 4

Click here to access/download;Figure;Figure 4.tif

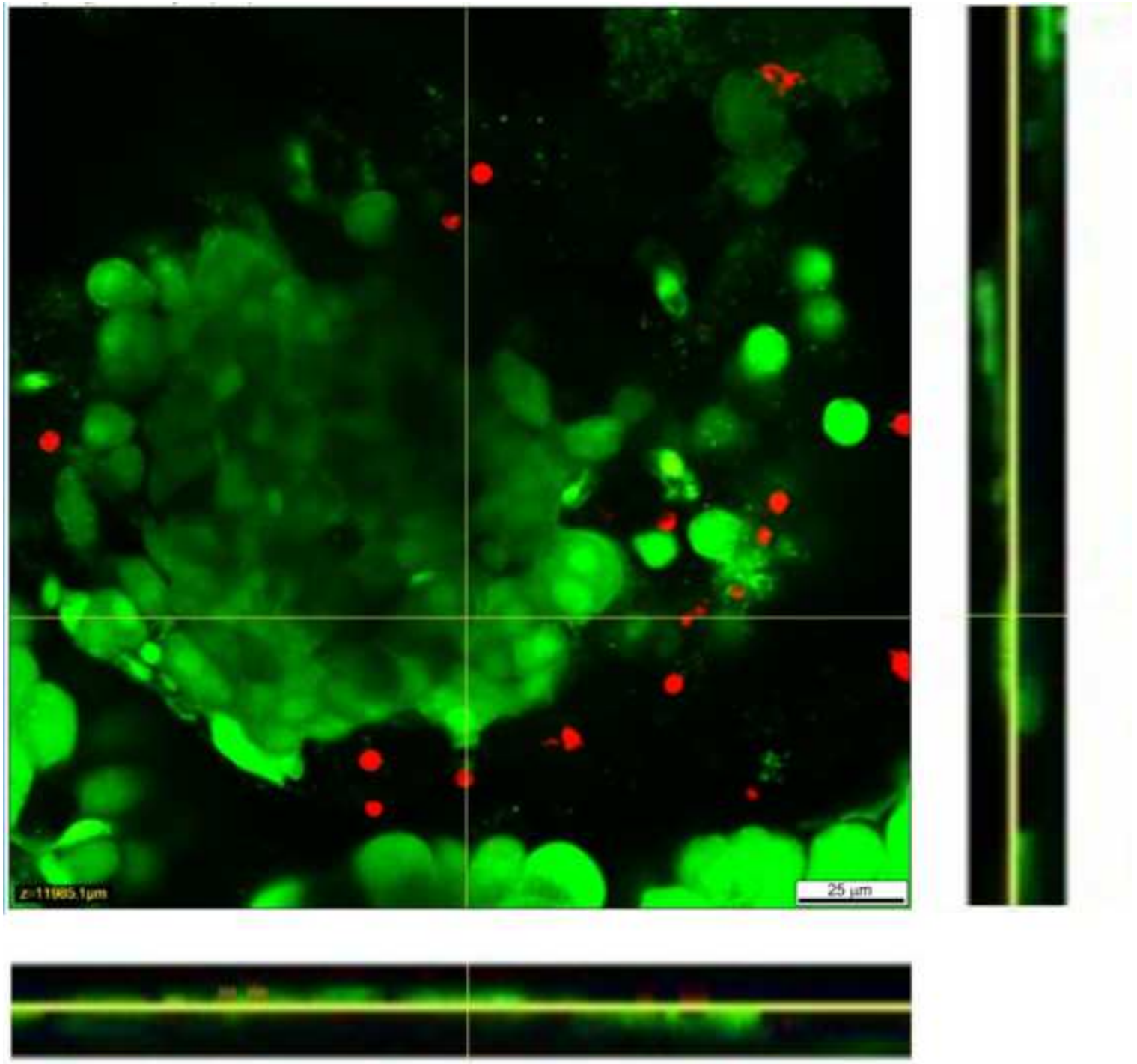

Figure 5

Click here to access/download;Figure;Figure 5.tif

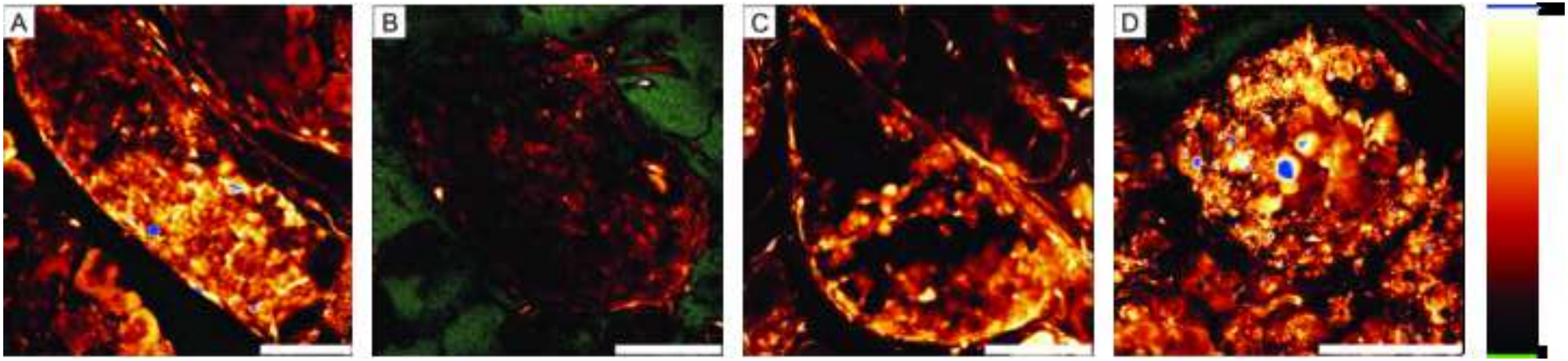

Figure 6

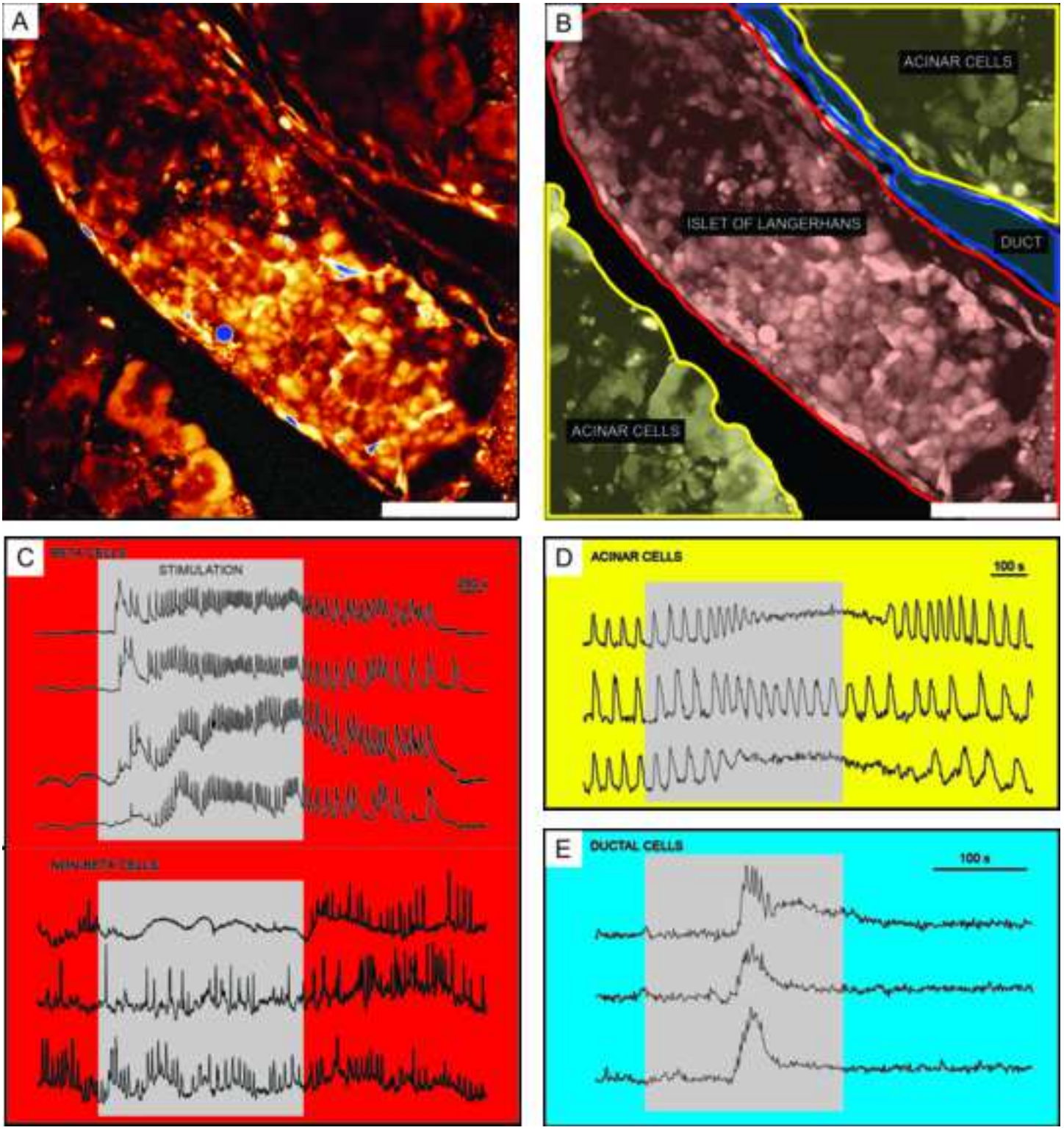

Figure 7

Click here to access/download;Figure;Figure 7_rev.tif

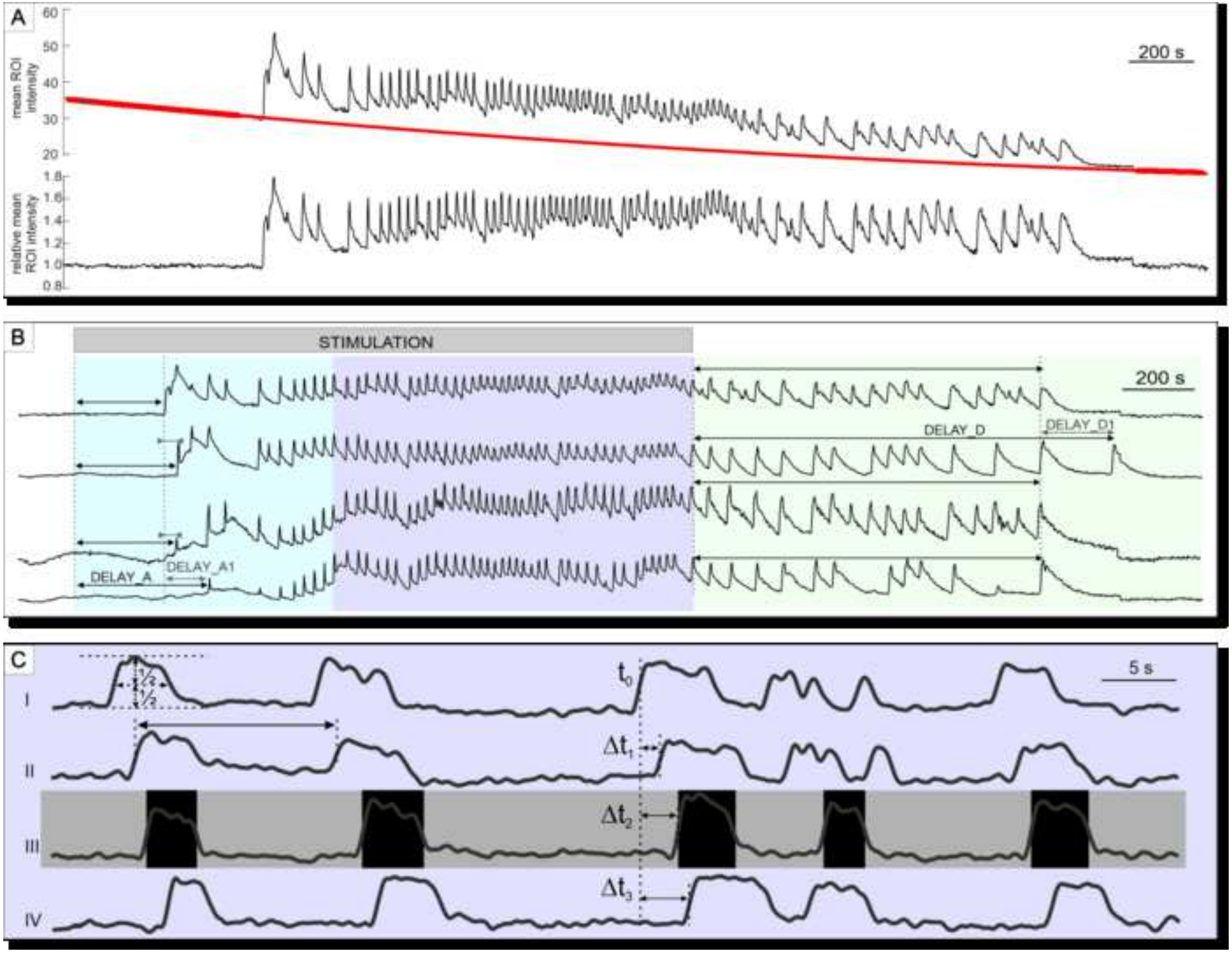

Table 1

Procedure step	Problem
Injection of agarose	Leakage of agarose into the duodenum
	Leakage of agarose out of the duct
	Incomplete agarose injection
Tissue slicing	The razor blade does not make clean cuts through tissue
	Pancreas tissue breaks out of agarose cubes
	Agarose cubes detach from the holder during slicing.
Live-dead assay	Poor signal
	Low viability
	Islets are difficult to identify
	Low signal

Calcium imaging	Poor signal-to-noise ratio
	The shape of the signal poorly detected
	Blurred image
	Islet looks destroyed
	Fast bleaching
	Phototoxicity observed
	No calcium response
	Mechanical drift
Analysis	No clear response is detected.
	Oscillations are detected only initially, during the beginning of the record.
	Detection of oscillations within an islet is taking very long (e.g., >1 h).

	A custom-made script suddenly stopped importing the data.

Cause
Incorrect clamping
Incorrect clamping
Perforation of the duct
Poor seal between syringe and duct
Early agarose solidification due to low agarose temperature
Too short an injection time
Damage of the common bile duct
Presence of accessory ducts that flow into the duodenum, kinks, or fibrosis in the duct system
Incomplete injection
Remnants of fat or connective tissue in the pancreas tissue
Incomplete injection or remnants of fat/connective tissue
Poor embedding
Blunt razor blade.
The cubes not glued properly.
Islets are not cut at the surface.
Incorrect settings of excitation/emission parameters
To high agarose temperature during injection
Degradation of tissue by exocrine tissue enzymes
Lack of experience, small islets, thick slices.
Islets are not cut at the surface and are therefore stained poorly
Incorrect setting of excitation/emission parameters

Incorrect settings
Islets not cut at the surface and therefore poorly stained
Too high a sampling frequency
Too low a sampling frequency
Incorrect phase
Too thick an optical plane
Too high agarose temperature during injection
Degradation of tissue by exocrine tissue enzymes
Incorrect focal plane
Incorrect settings
Emission detection is not set to the optimal wavelenghts.
Too high a sampling frequency
Incorrect stimulation
Phototoxicity
Dead cells
High tension between tubing/cables and microscope stage
Liquid leakage or changes in liquid volume in the recording chamber
Slice is not immobilized well
ROIs are including several cells.
ROIs are not set to pick up signal from cells.
Poor signal-to-noise ratio of the recording.
The threshold for detection is set too high.
If filtering was applied, the filtering distorted the oscillations.
Photobleaching of the signal.
Many data points are analyzed if high frequency and long records were used.

Update of the confocal system and the manufacturer changed the exporting protocol.

Solution
Make sure that the common bile duct is clamped at the papilla of Vater. Reposition/tigthen the clamp if necessary.
Place the clamp in such a way that the duodenum will be clamped as well, both proximally and distally from the papilla.
Make sure that the clamp at the papilla of Vater did not damage/perforate the duct
Try to cannulate the duct again closer to the duodenum and use forceps to keep the needle in place.
Find a better-suited needle or place a ligature.
Ensure that the solution's temperature is 37 °C or slightly more and inject the agarose as fast as possible.
Prolong the injection time or use more power when injecting
Try to cannulate the duct again closer to the duodenum and use forceps to keep the needle in place.
In small/young animals with narrow ducts use smaller-diameter needles (e.g., 32 G).
Use the well-injected part, try to gently elevate the pancreas during injection with your free hand (or ask a colleague for assistance) once the needle is safe in place in the duct lumen, use another mouse.
Decrease the slicing speed, stop slicing after each round and use scissors to cut slices carefully away from agarose block, if they are still attached
Further clean the tissue blocks from fatty/connective tissue and reinsert them in new agarose blocks, prepare new cubes using a new mouse
Re-embed tissue blocks and try again; make sure blocks of tissue are fully submerged in agarose and the agarose cubes are properly glued on a vibratome plate; make sure that the tissue blocks are dry before inclusion in agarose – try placing them on paper tissue before putting them in agarose.
Always use a new and sharp razor blade, degrease razor blade in acetone; use as thin a razor blade as possible,
Take care that proper amount of glue is applied. Apply some small amount of glue also on the side of agarose cubes.
Use slices with islets that are located closer to the slice surface to increase the chances of cutting through islet.
Follow manufacturer instruction.
Make sure to use the agarose solution at 37 °C.
After injection, maintain the tissue cooled; try to be as fast as possible
Try to find islets of Langerhans first under the stereomicroscope. In rat and human slices, where finding an islet can be especially difficult, dithizone staining can be used to gain experience in islet identification.
Use slices with islets on the top of the slice to increase the chances of islet cut-off, flip the slice around to check the other side, use another slice if needed.
Choose the correct laser, adjust laser power, recheck settings of emission detection window.

Optimize the signal-to-noise ratio by adjusting the laser power, detector amplification, and line averaging/binning; adjust the focal plane; use a resonant scanner if possible.
Use slices with islets that are located closer to the slice surface to increase the chances of islets being cut; flip the slice to check for a cut islet on the opposite tissue slice surface; use another slice if needed.
Decrease sampling frequency if applicable; set an interval between consecutive point illumination
Increase sampling frequency.
Correct phase of the bidirectional scanner
Decrease the pinhole to reduce optical plane thickness
Make sure to use the agarose solution at < 45 °C
After injection, maintain the tissue cooled; try to be as fast as possible, regularly exchange the storing solution.
Adjust the focal plane of the recording to about 15 µm below the cut surface.
Decrease laser power and increase gain, adjust the sampling frequency.
Adjust the emission detection window to the optimal values.
Decrease sampling frequency if applicable; allow an interval between consecutive point illumination.
Use proper stimuli for a given cell type, recheck that the perifusion fluid is flowing into the chamber.
Decrease sampling frequency if applicable; allow an interval between consecutive point illumination.
Use another islet, acinus, or duct.
Check the tubing.
Avoid droplets in perifusion; make sure both the inlet and the outlet contact the liquid; set the inflow and outflow to the same velocity.
Use a U-shaped platinum weight with a nylon mesh, check that the threads are taunt, replace if necessary.
Recheck ROI position on the reference high resolution image or by replaying time-lapse video.
Recheck ROI position on the reference high resolution image or by replaying time-lapse video.
Apply a filter to improve signal-to-noise ratio. Record the experiment again (see above).
Decrease the threshold for detection.
Recheck the filtering parameters and repeat the detection.
Recheck if the correction for the bleaching was applied correctly. Repeat experiment while taking care to avoid photobleaching.
Use parallel processing to maximize analyzing power.
Batch process the tasks.

Contact the manufacturer and ask for description of the exporting protocol.

Table of Materials

Name of Equipment	Company	Catalog Number	Comments/Description
Analytical balance KERN ALJ 120-4	KERN & SOHN GmbH	ALJ 160-4A	
Confocal microscope Leica TCS SP5 II Upright setup	Leica	5100001578	
Confocal microscope Leica TCS SP5 AOBS Tandem II setup	Leica		
Cork pad 15 cm x 15 cm			
Corning 15 mL centrifuge tubes	Merck KGaA, Darmstadt, Germany	CLS430790	
Corning Round Ice Bucket with Lid, 4 L	Fischer Scientific, Leicestershire, UK	432124	
Double edge razor blade	Personna, USA		
Dumont #5 - Fine Forceps	FST, Germany	11254-20	
Eppendorf Safe-Lock Tubes 0.5 mL	Eppendorf	0030 121.023	
Erlenmeyer flask 200 mL	IsoLab, Germany	027.01.100	
Fine Scissors - ToughCut	FST, Germany	14058-11	
Flat orbital shaker IKA KS 260 basic	IKA	Ident. No.: 0002980200	
Glass lab bottle 1000 mL	IsoLab, Germany	091.01.901	
Hartman Hemostat, curved	FST, Germany	13003-10	
HCX APO L 20x/1.00 W HCX APO L (water immersion objective, 20x, NA 1.0)	Leica	15507701	
Measuring cylinder 25 mL	IsoLab, Germany	015.01.025	
Micromanipulator Control box SM-7, Keypad SM-7	Luigs & Neumann	200-100 900 7311, 200-100 900 9050	
Microwave owen	Gorenje, Slovenia	MO20MW	
Osmometer Gonotec 010	Gonotec, Berlin, Germany	OSMOMAT 010 Nr. 01-02-20	
Paint brush	Faber-Castell, No.2		Any thin soft round paint brush No.2, preferably black
Paper towels			
Perifusion pumps	Ismatec	ISM 827	Reglo Analog MS - 4/8
Petri dish 100/20 mm	Sarstedt	83.3902	
Petri dish 35/10 mm	Greiner bio-one	627102	
Petri dish 35 x 10 mm Nunclon Delta	Thermo Fischer Scientific, Waltham, MA USA	153066	NON-STICKY for agarose blocks
pH meter inoLab pH Level 1	WTW, Weilheim, Germany	E163694	
Pipette 1000 mL	Eppendorf	3121 000.120	
Pipette 50 mL	Eppendorf	3121 000.066	
Push pins 23 mm	Deli, Ningbo, China	E0021	
Screw cap tube, 15 mL	Sarstedt	62.554.502	
Semken Forceps	FST, Germany	11008-13	
Stabilizing ring for Erlenmeyer flask	IsoLab, Germany	027.11.048	
Stereomicroscope Nikon SMZ 745	Nikon, Melville, NY USA		
Syringe Injekt Solo 5 mL	Braun, Melsungen, Germany	4606051V	
Syringe needle 0.30 x 12 mm (30 G x 1/2")	Braun, Melsungen, Germany	4656300	

Temperature controller	Luigs & Neumann	200-100 500 0150, 200-150-500-145	Slice mini chamber, Temperature controller TC 07
Tubings for perifusion system	Ismatec	SC0310	Ismatec Pharmed 1.14 mm(ID) + silicone tubing 1.0 (ID) x 1.8 mm(OD)
Ultrasonic bath Studio GT-7810A	Globaltronics		
Vibrotome Leica VT 1000 S	Leica, Nussloch, Germany	14047235613	
Volumetric flask 1000 mL	IsoLab, Germany	013.01.910	
Vortex mixer Neolab 7-2020	Neolab	7-2020	
Water bath Thermo Haake open-bath circulator	Thermo Fisher Scientific	Z527912	

Name of Material/Reagent	**Company**	**Catalog Number**	**Comments/Description**
Calcium chloride dihydrate - $CaCl_2.2H_2O$	Sigma Aldrich, Germany	C5080-500G	
D-(+)-glucose	Sigma Aldrich, Germany	G8270-1KG	
Dimethyl sulfoxide	Sigma Aldrich	D4540-100ML	
DL-lactic acid	Sigma Aldrich, Germany	L1250-500ML	
Dulbecco's Phosphate Buffered Saline	Merck KGaA, Darmstadt, Germany	D8662-500ML	
Gas mixture containing 95% O_2 and 5% CO_2 at barometric pressure			
Glue Wekem sekundenkleber WK-110	Wekem GmbH, Bergkamen, Germany	WK 110-020	
HEPES	Sigma Aldrich, Germany	H3375-250G	
L-(+)-ascorbic acid	Sigma Aldrich, Germany	A9,290-2	
LIVE/DEAD Viability/Cytotoxicity Kit, for mammalian cells	Thermo Fischer Scientific, Waltham, MA USA	L3224	
Magnesium chloride hexahydrate - $MgCl_2.2H_2O$	Sigma Aldrich, Germany	M2670-500G	
Myo-inositol	Sigma Aldrich, Germany	I5125-100G	
Oregon Green 488 BAPTA-1, AM	Invitrogen (Thermo FisherScientific)	O6807	cell-permeable Ca^{2+} indicator (excitation/emission: 495/523 nm)
Pluronic F-127 (20% Solution in DMSO)	Invitrogen (Thermo Fisher Scientific)	P3000MP	polaxamer: nonionic triblock copolymer
Potassium chloride - KCl	Sigma Aldrich, Germany	31248	
SeaPlaque GTG agarose	Lonza, Rockland, USA	50111	
Sodium bicarbonate - $NaHCO_3$	Honeywell, Germany	31437-500G	
Sodium chloride - NaCl	Honeywell, Germany	31434-1KG	
Sodium hydroxide - NaOH	Sigma Aldrich, Germany	30620	
Sodium phosphate monobasic- NaH_2PO_4	Sigma Aldrich, Germany	S0751-500G	
Sodium pyruvate	Sigma Aldrich, Germany	15990-100G	

Name of Software	**Company**	**Catalog Number**	**Comments/Description**
FIJI			FIJI is an open source project
LASAF	Leica microsystems, Inc.		
Matlab	Mathworks		
Python	Python Software Foundation		Python is an open source project

Maribor, February 1st 2021

Dear Doctor Vidhya Iyer,

We would like to thank you for considering our manuscript for publication in JoVE. We thoroughly studied your and reviewers´ comments and, whenever possible, changes were made to the manuscript to incorporate the suggestions and address issues raised by reviewers. All text changes are marked using the MS Word track changes function.

We hope that the revised version of our manuscript will meet the reviewers´ expectations and also meet the quality demands of your fine journal. Finally, we authors would like to sincerely thank you and the reviewers for comments that helped us further improve the quality of our manuscript and thus, hopefully, increase its reach and impact.

Please find below our point-by-point responses.

With kind regards,

Andraž Stožer, Jurij Dolenšek, Lidija Križančić Bombek, Viljem Pohorec, Marjan Slak Rupnik, and Maša Skelin Klemen

Editorial comments:

1. Please take this opportunity to thoroughly proofread the manuscript to ensure that there are no spelling or grammar issues.

We read the manuscript and corrected the detected issues.

2. Please provide an institutional email address for each author.

We added the institutional email addresses.

3. Please include an ethics statement before your numbered protocol steps, indicating that the protocol follows the animal care guidelines of your institution.

We added the ethics statement in the revised manuscript.

4. Please adjust the numbering of the Protocol to follow the JoVE Instructions for Authors. For example, 1 should be followed by 1.1 and then 1.1.1 and 1.1.2 if necessary. Please refrain from using bullets or dashes.

We adjusted the numbering.

5. Please add more details to your protocol steps. Please ensure you answer the “how” question, i.e., how is the step performed? Alternatively, add references to published material specifying how to perform the protocol action.

The text was rephrased to emphasise the ‘how’ question, as suggested by the editor.

6. Line 123: Please include more details regarding the osmolarity measurements. How is it performed?

We included more details about the osmolarity measurements.

7. For SI units, please use standard abbreviations when the unit is preceded by a numeral, throughout the protocol. Abbreviate liters to L to avoid confusion. For time units, use abbreviated forms for durations of less than one day when the unit is preceded by a numeral. Do not abbreviate day, week, month, and year. Examples: 5 h, 10 min, 100 s, 8 days, 10 weeks, 10 mL, 8 µL, 7 cm2

We corrected SI units as suggested.

8. Line 184-186: Please include the volume of ice cold ECS used. Is there any specific temperature for cooling? How much volume of ECS is used for washing?

We specified the volume of ECS used for these preparation steps.

9. Line 287-293/301-336: The Protocol should be made up almost entirely of discrete steps without large paragraphs of text between sections. Please simplify the Protocol so that individual steps contain only 2-3 actions per step and a maximum of 4 sentences per step.

We much appreciate this constructive remark. The appropriate section was rephrased and simplified as suggested.

10. JoVE cannot publish manuscripts containing commercial language. Please remove all commercial language from your manuscript and use generic terms instead. All commercial products should be sufficiently referenced in the Table of Materials: e.g., Matlab, Python, etc. We must maintain our scientific integrity and prevent the subsequent video from becoming a commercial advertisement.

We removed all commercial language in the manuscript as suggested by the editor.

11. Please include a one line space between each protocol step and highlight up to 3 pages of protocol text for inclusion in the protocol section of the video. This will clarify what needs to be filmed.

We included line space as suggested and marked 3 pages of protocol for video.

12. Please do not use any abbreviations for journal titles and book titles. Article titles should start with a capital letter and end with a period and should appear exactly as they were published in the original work, without any abbreviations or truncations.

We corrected the citations accordingly.

13. Please remove trademark (™) and registered (®) symbols from the Table of Equipment and Materials.

We removed trademark and registered symbols.

Reviewer #1:

Manuscript Summary:

The manuscript describes calcium imaging of pancreas tissue slices, a difficult yet valuable technique that has several advantages over similar options (e.g. imaging of isolated islets). The methodology is detailed with clear supporting figures, as well as extra tips and a clear troubleshooting section. In some areas, more detail and clarity could be given.

We are pleased that the reviewer has recognized our work as valuable. We revised some sections of the manuscript to provide more details and clarify the methodology, which we hope will improve the quality of our manuscript.

Minor Concerns:

Section 1:

In 1.1, providing storage conditions for the different solutions would be useful (e.g. temperature and length of time). Also recommended volumes to make up. Protocl for bubbling with carbogen should go into more detail for people who are unfamiliar with this process. For the 10x STOCK of ECS, 'When the extracellular buffer is needed mix 100ml of STOCK with 2ml of 1M CaCl2, 1ml of 1M MgCl2, 0455 ml lactic acid and 1.08g glucose...'. Mention what volume of water is needed to dilute to a 1x solution.

We specified the storage condition, volumes for preparation of the solutions and explained the protocol for carbogen usage as suggested.

In 1.2, step 1, explain how the syringe is placed in the water bath, how is it contained? In step 8, clarify how much ice cold ECS needs to be poured on? what volume?

All the questiones were addressed and volume specified.

In 1.3, specify the recommended number of ECS ice cubes?

We specified the number and the volume of ice cubes as suggested.

Are sections 1.2 and 1.3 unique for performing imaging or can they be used for other assays? I assume they can be but would be good to confirm as groups may want to run Ca2+ imaging alongside secretion/structural studies on tissue slices from the same mouse.

We are thankful for this remark. Pancreas tissue slices could also be used for in electrophysiological, secretion, and structural studies and we pointed this out in the revised version of the manuscript.

Section 3:

Step 3 could be combined with step 2, as I assume the ambient air and shielding from light is for the 50 min on the shaker.

The reviewer is correct. We combined these two steps.

Section 4:

In 4.2, specify recommended volume in the chamber, also clarify what 'meander cutoff' means? Any recommendation for optimal imaging solution? Suggested speed of perifusion would also be useful given potential for drift if too fast.

The volume is specified, and the meandering of the flow within the recording chamber is rephrased. Optimal solution were referenced in the solutions section, and the perifusion speed was specified, as suggested by the reviewer.

Generally, a figure of the imaging setup including chamber, perifusion system and a depiction of how the tissue is immobilized with the nylon mesh and weight would be useful, as it is difficult to interpret via text.

This is a great, constructive remark. A schematic pictogram of the recording chamber, perifusion sistem and the sistem for tissue slice immobilization was added to the figure 1 into the panel entitled calcium imaging, as suggested by the reviewer.

Representative results:

In figure 6c lower panel, I can see no decrease of activity in any of the traces despite it being stated in the text here, '... while non-beta cells will respond to glucose stimulus with faster irregular oscillations or a decrease in activity...', I understand you may be referring to the literature here but was this also observed in your study?

We agree with the reviewer. Putative non-beta cell traces were selected in a way that could confuse readers. For practical purposes (in order not to draw a completely new Figure 6) we replaced the traces with more stereotypical non-beta cell responses from the same islet, i.e., we replaced them with a cell that clearly shows less activity under high glucose conditions, and two cells whose activity was not clearly glucose-dependent. More importantly, since the protocol used in this stimulation was designed to detect beta cells activity, further discrimination of non-beta cells is not possible. In the revised version, we explicitily point this out in many different parts of the manuscript. For readers interested in calcium imaging of non-beta cells, we have revised and rewritten the appropriate sections in the discussion, where we highlighted the relevant discriminatory protocols for non-beta cells. We also briefly addressed the issue of PP and epsilon cell identification and suggested some additional protocols for ductal cells. Accordingly, a number of additional relevant rerefences were added.

Discussion:
Specify why recovery period is needed for islets and not for tissue slices. Expand more on the negatives of this technique, what exactly about the isolation procedure is detrimental to cellular function? Does processing tissue in this way has some deleterious effects that may not be occur in isolated islets?

This is a very important and complex issue. We totally agree and are very thankful that this was brought up. In the revised version, we systematically included and describes many more shortcomings of the tissue slice. We also specifically but briefly addressed the topic of culturing isolated islets, specifically in the context of calcium imaging. To keep things fair, we also additionally addressed the future possibility that slices be cultured for longer periods of time.

For the sentence, 'To discriminate alpha cells functionally, low (3mM) glucose, glutamate, or adrenaline can be used...' reference Cabrera et al, 2008 Cell (https://pubmed.ncbi.nlm.nih.gov/18522835/) and Hamilton et al, 2019, JoVE (https://www.jove.com/t/59491/imaging-calcium-dynamics-subpopulations-mouse-pancreatic-islet)

References were cited as suggested by the reviewer.

General comments:

Petri dishes referred to by size and volume, choose one. If you want to specify volume of a solution in a petri dish say for example '100mm petri dish containing 60ml HBS...'

Petri dishes are referred by size, and the volume of a solution is specified.

Figure resolution could be improved.

We improved figure resolution as much as possible.

Reviewer #2:

The manuscript by Stozer et al. described a very useful technique for the study of islet or pancreas physiology, using live cell imaging with mouse pancreas tissue slices. Authors explained the rational and usefulness of the technique and detailed the experimental protocol. The manuscript could be followed quite easily for researchers in the field and it would be possible to implement the technique, if equipment is available.

We are pleased that the reviewer has recognized our work as useful.

I have only a few minor comments as follows:

1. For dissection of the mouse and ductal injection, authors should mention the use of a dissecting microscope. Although the procedure is straightforward, the part for ampulla of Vater clamping and later agarose will definitely need a dissecting microscope.

We much appreciate that the reviewer drew our attention to this missing part of the described protocol. In the revised version of the manuscript, we pointed out that a dissecting microscope is an essential part of the equipment needed to prepare the pancreas tissue slices successfully.

2. Line 175. 'hardly' be changed to hard.

Corrected.

3. For 1.3.3 - it should be mentioned that once the slices have been collected, how one should preserve the slices before experiments/further treatments

The appropriate section was revised with detailed instructions.

4. Line 215. Does the 'Figure 3' here mean Figure 4?

We agree and have renumbered the figure accordingly.

5. Authors explained that when setting up imaging, one should optimise 'the signal-to-noise ratio'. What is the typical pin hole setting?

We revised the manuscript as suggested by the reviewer.

6. I am not convinced by the representative traces in Fig 6C for non-beta cells. The response looked more like less typical beta cells. Additional functional identification is needed - such as adrenaline for alpha cells and beta cells, ghrelin for delta cells.

We totally agree that the putative non-beta cell traces were selected in a way that could confuse readers. For practical purposes (in order not to draw a completely new Figure 6) we replaced the traces with more stereotypical non-beta cell responses. We additionally clearly pointed out at many points in the article that a simple square-pulse glucose stimulus is unable to specifically functionally identify non-beta cells (in caption and in discussion), and suggested many different solutions to this problem. As this is a highly relevant issue and was also raised by the other two reviewers, please see also our responses to them.

7. The resolution of figures is a bit low. Some fonts are hard to read.

We improved figure resolution as much as possible.

8. What is the model of the confocal microscope? What is the acquisition software? It may be the authors tend to provide a general guidance for the technique, but with certain examples can make it easier to follow.

The model and the imaging software are referenced in the Table of Materials in the revised version, to comply with the reviewers comment and meet editorial policy. A specific example and reference to the Leica confocal upright system with the LASAF imaging software is referenced in the table, as suggested by the reviewer.

9. The final table can be re-organised. It can be divided into 'equipment' and 'reagents' and authors may consider adding software too. The current form is a little messy.

We agree and have reorganized the table accordingly.

10. I don't quite understand the 'comments/description' part.

We revised the table and included only the relevant information in the table's comments/description part.

Reviewer #3:

I think this is an extremely important and useful article. I highly recommend its publication.

We sincerely acknowledge the effort of the reviewer for evaluating our work, and we are pleased that our work was recognized as extremely important and useful.

I have a few minor comments/questions:

-I am unsure why significant parts of the text were highlighted in yellow.

We followed the editor's instructions and highlighted 3 pages of protocol text for inclusion in the protocol section of the video.

-table of materials needs checking for formatting- extends over multiple pages

Thank you. We revised and formatted the table accordingly.

-figure 7 - indicate glucose levels corresponding to stimulated and unstimulated state

Glucose levels were specified as suggested.

-figure 6 - its unclear how beta cells and non-beta cells are distinguished. This is a critical point.

In the revised version, we corrected Figure 6 and its caption to clearly point out that a simple square-pulse glucose stimulus is unable to specifically functionally identify non-beta cells (in caption and in discussion), and suggested many different solutions to this problem. As this is a highly relevant issue and was also raised by the other two reviewers, please see also our responses to them.